SKB

TECHNICAL REPORT 97-15

Dissolution studies of synthetic soddyite and uranophane

Ignasi Casas[1], Isabel Pérez[1], Elena Torrero[1],
Jordi Bruno[2], Esther Cera[2], Lara Duro[2]

1 Dept. of Chemical Engineering, UPC
2 QuantiSci SL

September 1997

SVENSK KÄRNBRÄNSLEHANTERING AB
SWEDISH NUCLEAR FUEL AND WASTE MANAGEMENT CO

P.O.BOX 5864 S-102 40 STOCKHOLM SWEDEN
PHONE +46 8 665 28 00
FAX +46 8 661 57 19

DISSOLUTION STUDIES OF SYNTHETIC SODDYITE AND URANOPHANE

Ignasi Casas[1], Isabel Pérez[1], Elena Torrero[1], Jordi Bruno[2], Esther Cera[2], Lara Duro[2]

1 **Dept. of Chemical Engineering, UPC**
2 **QuantiSci SL**

September 1997

Dissolution studies of synthetic soddyite and uranophane

Ignasi Casas, Isabel Pérez, and Elena Torrero.

Dept. of Chemical Engineering, UPC.

Jordi Bruno, Esther Cera and Lara Duro

QuantiSci SL.

ABSTRACT

The dissolution of synthetically obtained soddyite and uranophane has been studied in solutions of low ionic strength. These are the likely final phases of the oxidative alteration pathway of uranium dioxide. The thermodynamic and kinetic dissolution properties of these phases have been determined at different bicarbonate concentrations.

The solubilities determined in the experiments with soddyite correspond fairly well to the theoretical model calculated with a log $K^0_{s0} = 3.9 \pm 0.7$. For uranophane, the best fitting was obtained for a log $K^0_{s0} = 11.7 \pm 0.6$.

The dissolution rate in the presence of bicarbonate gave for soddyite an average value of 6.8 ($\pm$4.4) 10^{-10} mol m^{-2} s^{-1}.

For uranophane, under the same experimental conditions, the following dissolution rate equation has been derived:

$$r_0 \text{ (mol m}^{-2}\text{ s}^{-1}) = 10^{-9 \pm 2} \cdot [HCO_3^-]^{0.69 \pm 0.09} \cdot [H^+]^{-0.1 \pm 0.2}$$

SAMMANFATTNING

Upplösningen av syntetiskt soddyit och uranofan har studerats i lågjonstyrkelösningar. Dessa två faser är möjliga slutfaser i de oxidativa omvandlingskedja av uranoxid. De termodynamiska och kinetiska upplösningsegenskaperna av dessa två faser har bestämts i olika bikarbonathaltiga lösningar.

De lösligheter som har bestämts i försök med soddyit stämmer ganska bra med den teoretiska modellen med log K^0_{s0} =3.9 ± 0.7. För uranofan erhålls den bästa anpassningen med log K^0_{s0} =11.7 ± 0.6.

Medelvärdet för upplösningshastighet av soddyit i närvaro av bikarbonat var 6.8 (± 4.4) 10^{-10} mol m^{-2} s^{-1}.

Under samma experimentella förhållande erhölls följande upplösningshastighetsuttryck för uranofan:

$r_0(\text{mol m}^{-2}\text{ s}^{-1}) = 10^{-9 \pm 2} [HCO_3^-]^{0.69 \pm 0.09} [H^+]^{-0.1 \pm 0.2}$

TABLE OF CONTENTS

SUMMARY

The dissolution of synthetically obtained soddyite and uranophane has been studied in leaching solutions with and without carbonate. The thermodynamic and kinetic dissolution properties of these phases have been determined at different bicarbonate concentrations. This uranium-silicate phases are expected to be a secondary solid phase of the oxidative alteration pathway of uranium dioxide in waters with low phosphate content and, consequently, they are likely to constitute the long-term uranium solubility limiting phases in average swedish granitic groundwaters.

The experiments were performed in solutions containing initial concentrations of silicon and calcium, with the aim of preventing precipitation of secondary phases. Despite this caution the experimental results obtained in the absence of bicarbonate have shown multiple processes of dissolution and precipitation taken place simultaneously. This has so far unabled an actual modeling of the experiments. In the presence of bicarbonate in the leaching solution, no precipitation of secondary phases has been detected for soddyite, and the results of this series of experiments are the ones described in the present report. For uranophane, the first experiments performed with bicarbonate showed the formation of secondary solid phases. For this reason, subsequent assays were performed using distilled water with the corresponding bicarbonate content. In these experiments no secondary phase formation was observed and these are the results considered in this study to extract thermodynamic and kinetic information for this phase.

The solubilities determined in the experiments with soddyite correspond fairly well to the theoretical model calculated with a $\log K^0_{s0} = 3.9 \pm 0.7$. For uranophane, the best fitting was obtained for a $\log K^0_{s0} = 11.7 \pm 0.6$.

On the other hand, the general trend of the total uranium in solution measured in the experiments with soddyite as a function of time has been fitted by using three different methodologies: ① by direct least-square of the initial linear trend of the data, ② by using a kinetic equation obtained from the principle of detailed balancing of the dissolution reaction, and ③ by the use of the EQ3/6 code. Comparable results were obtained in the different modeling exercises. Taking into account the similarity of the behavior observed in the series of experiments performed and also due to a larger complexity of the data treatment, for uranophane only the methodology number ① has been used.

The dissolution rate in the presence of bicarbonate, normalized to the total surface area used in the experiments as measured with the BET method, gave for soddyite an average value of 6.8 ($\pm$4.4) 10^{-10} mol m^{-2} s^{-1}.

For uranophane, under the same experimental conditions, a clear dependence of the initial rate of dissolution on both bicarbonate and pH has been found, and a dissolution rate equation has been derived:

$$r_0 \text{ (mol m}^{-2}\text{ s}^{-1}) = 10^{-9 \pm 2} \cdot [HCO_3^-]^{0.69 \pm 0.09} \cdot [H^+]^{-0.1 \pm 0.2}$$

1 INTRODUCTION

The performance assessment of HLNW repositories requires the long-term description of the behavior of the waste matrix. This is basically done by using the experience from leaching experiments of actual spent fuel to derive kinetic and thermodynamic models for the dissolution of spent fuel under repository conditions.

However, the time scales of spent nuclear fuel dissolution experiments is of the order of 2 to 10 years, while the performance of a spent fuel repository should be assessed for much longer times (10^5 -10^6 years). These time scales can be bridged using appropriate natural systems that give insight into the critical steps for the oxidative alteration of spent fuel in granitic environments.

Recently, much attention has been devoted to the mineralogical and crystallographic studies of the pathways of uraninite alteration and the consequences on the long-term stability of spent fuel (Finch and Ewing 1989, 1991, 1992; Janeczek and Ewing, 1992). In order to better understand the natural complexity, the systematic study of the dissolution behavior of uranium phases is important. Previous studies (Casas et al., 1994) have demonstrated the complexity of the studies carried out using natural samples. The results have been in some cases of difficult evaluation even considering the careful leaching studies performed as well as the extensive characterizations of the solid phase before and after the dissolution experiments. For this reason, a series of experiments has been started where uranium solid phases have been synthetically obtained under well controlled laboratory conditions.

In the present work, the kinetic and thermodynamic models obtained to describe the dissolution behavior of synthetic soddyite and uranophane are presented.

2 EXPERIMENTAL

2.1 SYNTHESIS OF URANYL SILICATE PHASES

The synthesis of the two solid phases followed the systematic proposed by Nguyen et al. (1992). Two batches were prepared for each solid synthesized from uranyl nitrate. All solid phases were treated in a glass Parr bomb to improve their crystallinity. Commercial reagents from Fluka, Merck and Panreac were used. It follows a summary of the synthesis procedure for each solid phase.

2.1.1 Synthesis from uranyl nitrate

Uranophane

Uranophane was prepared by reacting aqueous carbonate-free solutions of uranyl nitrate [A: (23.4 g (45.6 mmol), 250 ml), B: (11.72 g (22.8 mmol), 150 ml)] sodium metasilicate [A: (8.3 ml (45.6 mmol), 150 ml), B: (4.20 g (22.8 mmol), 100 ml)] and calcium acetate [A: (3.65 g (22.8 mmol), 50 ml), B: (1.82g (11.4 mmol), 20 ml)]. The pH of the reaction mixture was adjusted to 8.0 by addition of carbonate-free sodium hydroxide.

The solution was stirred for 4 hours before being refluxed at 363 K for 24 hours. Then, it was filtered and the precipitate was washed several times with boiling deionized water.

The solid was dried under vacuum and homogenized. Then, it was transferred to a glass Parr bomb and reacted with water (150 ml) at 391 K for two weeks.

The product was filtered and vacuum-dried overnight. The yield was 16.21 g (82.9%) for batch A and 6.25 g (63.84%) for batch B.

Soddyite

A solution of uranyl nitrate (15.22 g, 29.6 mmol) in water (200 ml) was added to an aqueous solution (50 mL) of sodium metasilicate (2.8 ml, 14.8 mmol). The pH of the reaction medium was different to the one described by Nguyen et al., because the starting chemical reagent was uranyl nitrate, instead of uranyl acetate as they described. Hence, the pH was adjusted to 4.5-5 by addition of 4.91 g of sodium acetate (batch A) and by addition of a concentrate solution of sodium hydroxide (batch B).

The mixture was reacted at room temperature for 100 hours. After this time, the reaction mixture was refluxed at 353 K for 6 hours. The solution was filtered and the precipitate was washed several times with boiling deionized water.

The precipitate was dried in an oven at 383 K for 24 hours and homogenized. Then, it was transferred to a glass Parr bomb and reacted with water (150 ml) at 403 K for two weeks. The product was finally washed with deionized water and vacuum-dried overnight. The yield was 1.58 g (15.91%) for batch A and 4.98 g (50.15%) for batch B.

2.1.2 Synthesis from uranyl acetate

Uranophane

Aqueous carbonate-free solutions of uranyl acetate (15.16 g (35.0 mmol), 300 ml), sodium metasilicate (7.66 g (35.0 mmol), 30 ml) and calcium acetate (2.80 g (17.5 mmol), 20 ml) were reacted at pH=8.8 with carbonate-free sodium hydroxide.

The reaction mixture was stirred for 4 hours at room temperature and refluxed at 363 K for two days.

The solid was filtered, washed several times with boiling deionized water and dried under vacuum overnight.

The product was transferred to a glass Parr bomb and reacted with water (150 ml) at 393 K for 18 days. After this time, it was filtered and vacuum-dried overnight. The final product was homogenized and the yield was 12.26 g (81.73%).

Soddyite

A solution (50 ml) of sodium metasilicate (4.91 g, 22.4 mmol) was added to a solution of uranyl acetate (19.43 g, 44.8 mmol) in water (650 ml) . The solution was stirred for half an hour. The pH of the reaction mixture was 4.95.

The volume of this solution was concentrated by evaporation at 253 K to approximately 200 ml. The solution was filtered and the precipitate was washed several times with boiling deionized water . The solid was vacuum-dried overnight. Then, it was transferred to a glass Parr bomb and reacted with water (150 ml) at 393 K for four weeks.

The product was washed with deionized water and vacuum-dried overnight. It was finally homogenized. The yield was 6.61 g (44.07%).

2.2 CHARACTERIZATION OF THE SOLID PHASES

Several methods were used for the characterization of the different solid phases. The analytical methods used were X-ray powder diffraction (XPD), Scanning Electron Microscopy (SEM), FTIR spectra and solid surface area (BET) determinations. In four of the synthesized uranium silicates the water content was determined thermogravimetrically. The results obtained by these techniques are presented below.

2.2.1 XPD

X-ray powder diffraction provides information about unit cells parameters, crystallinity and identification of the phase or phases contained in the bulk of the sample. The insensitivity of XPD to phases which are present in amounts less than approximately ten volume percent makes the identification of minor phases difficult.

The diffraction patterns of the synthetic uranyl silicates were taken with the Cu K α radiation using a typical wavelength of 1.5418 Å on a wide-angle Siemmens D-500 equipped with a quartz primary and graphite secondary monochromator. The database of the powder diffraction standard was the JCPDS (Joint Committee of Powder Diffraction Standard).

The X-ray diffraction patterns were performed at different times of the synthesis procedure for each solid phase, because the first analysis performed showed a poorly crystallized solid phase (broad bands in the peak positions). The diffraction patterns obtained for the two batches (A and B) of uranophane are presented below, together with the theoretical pattern found in the bibliography (Figure 2-1 and Figure 2-3).

The X- ray diffractogram obtained after two weeks of treatment showed that the crystallinity of the solid had significantly increased, giving sharper peaks in the diffraction pattern (Figures 2-2 and 2-4).

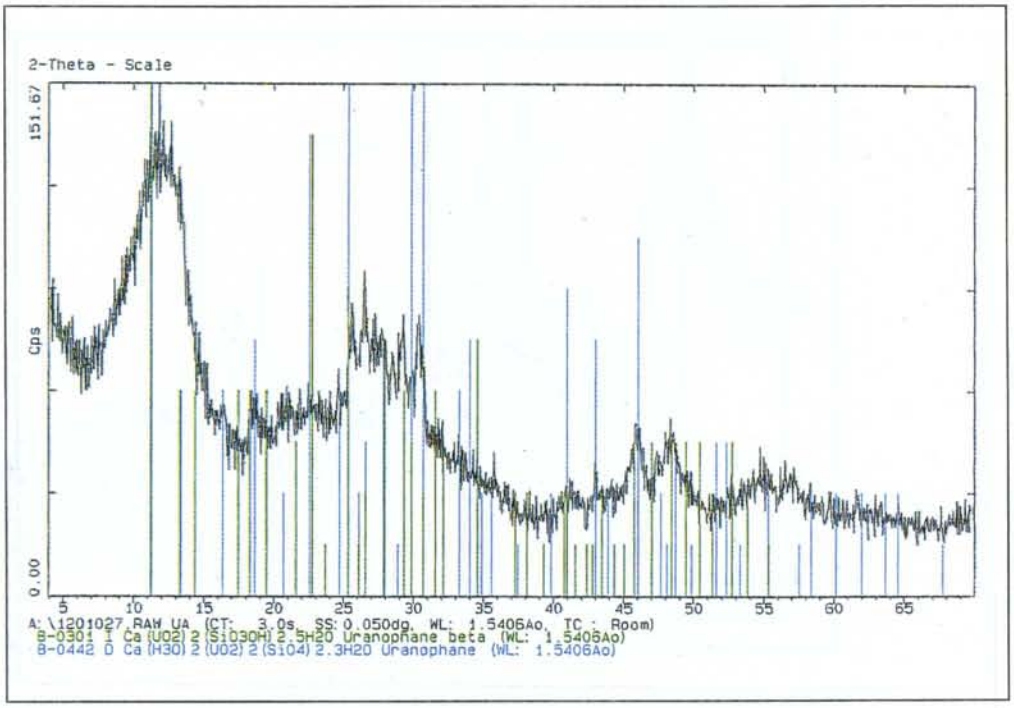

Figure 2-1. *X-ray powder-diffraction pattern of synthetic uranophane (batch A). After one week of treatment to improve its crystallinity.*

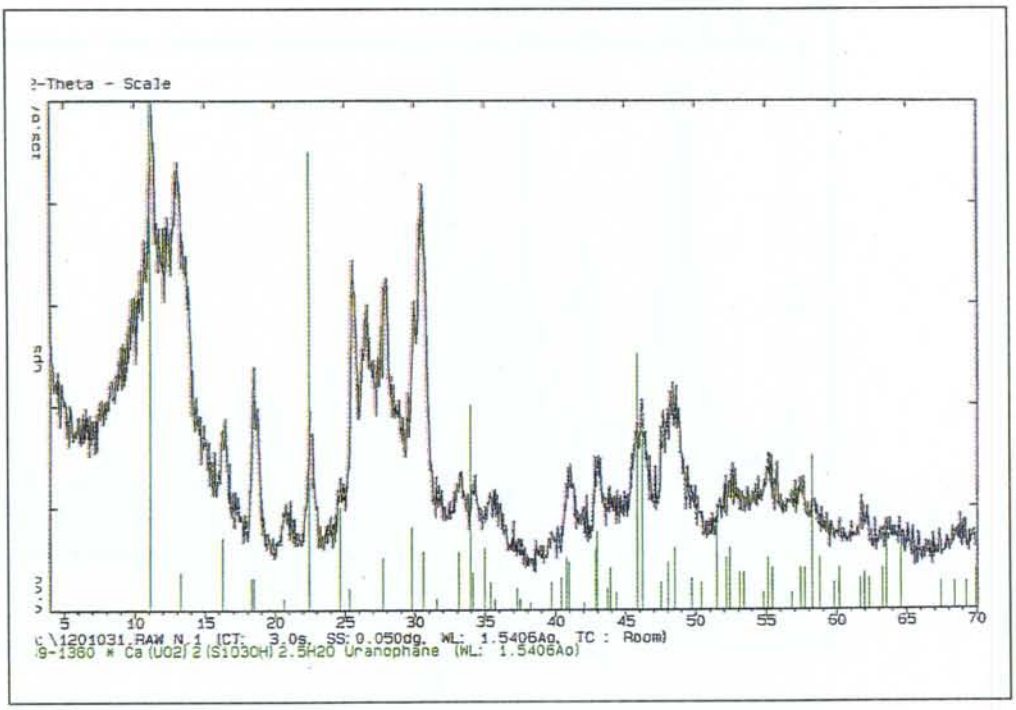

Figure 2-2. *X-ray powder-diffraction pattern of synthetic uranophane (batch A).After two weeks of treatment to improve its crystallinity.*

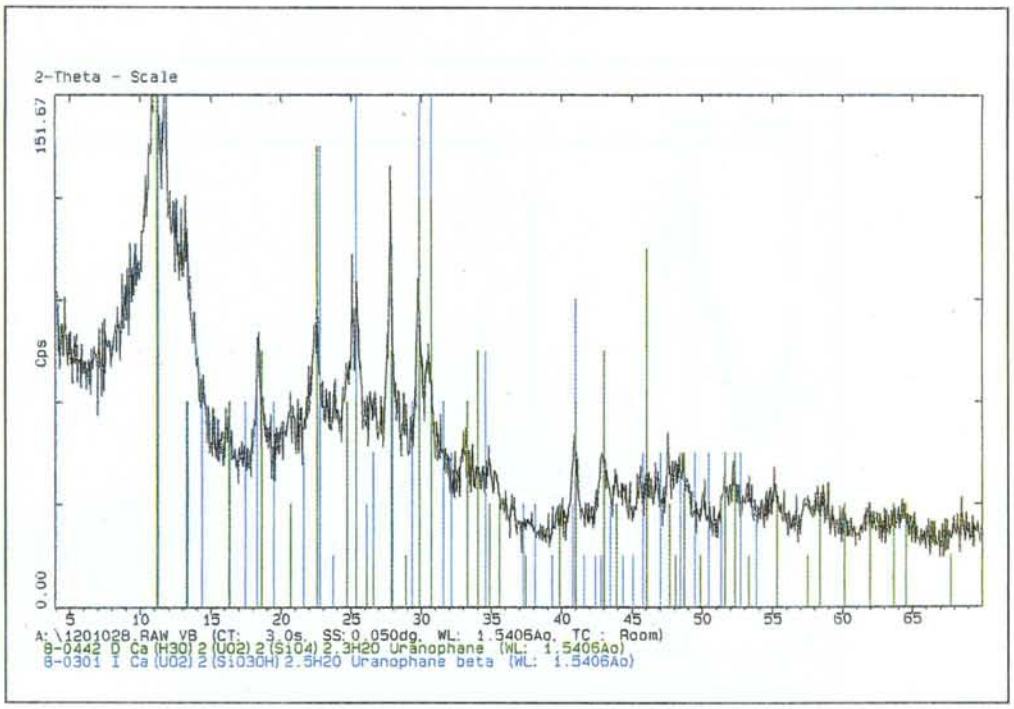

Figure 2-3. *X-ray powder-diffraction pattern of synthetic uranophane (batch B). After one week of treatment to improve its crystallinity.*

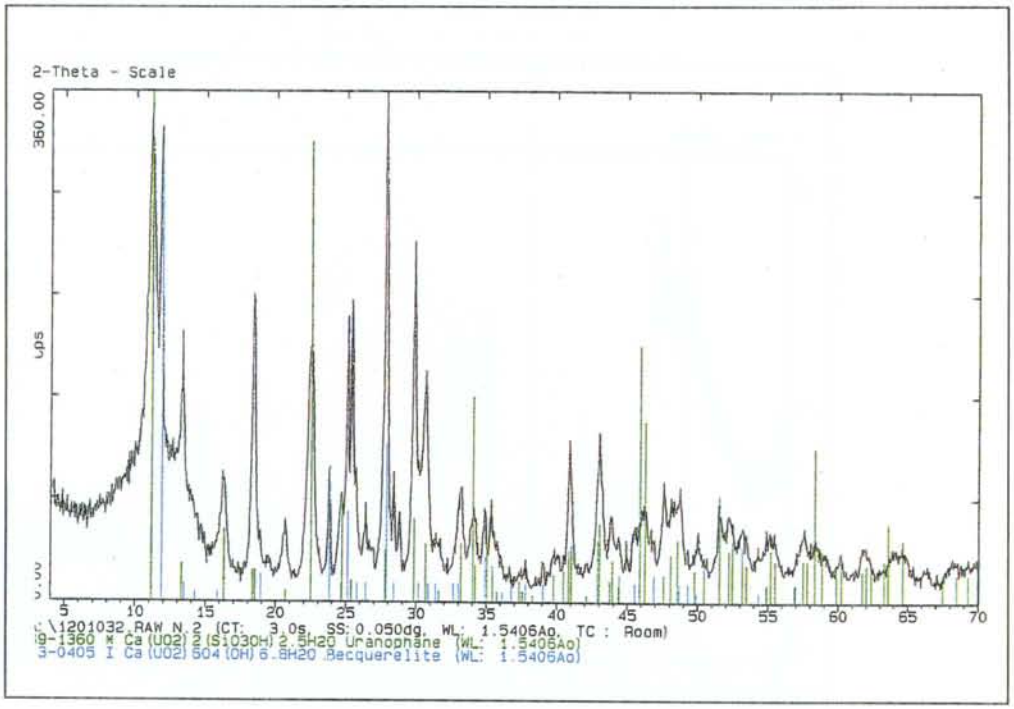

Figure 2-4. *X-ray powder-diffraction pattern of synthetic uranophane (batch B). After two weeks of treatment to improve its crystallinity.*

The increase of the solid crystallinity after the treatment is better observed for the synthetic soddyite (Figures 2-5, 2-6, 2-7 and 2-8).

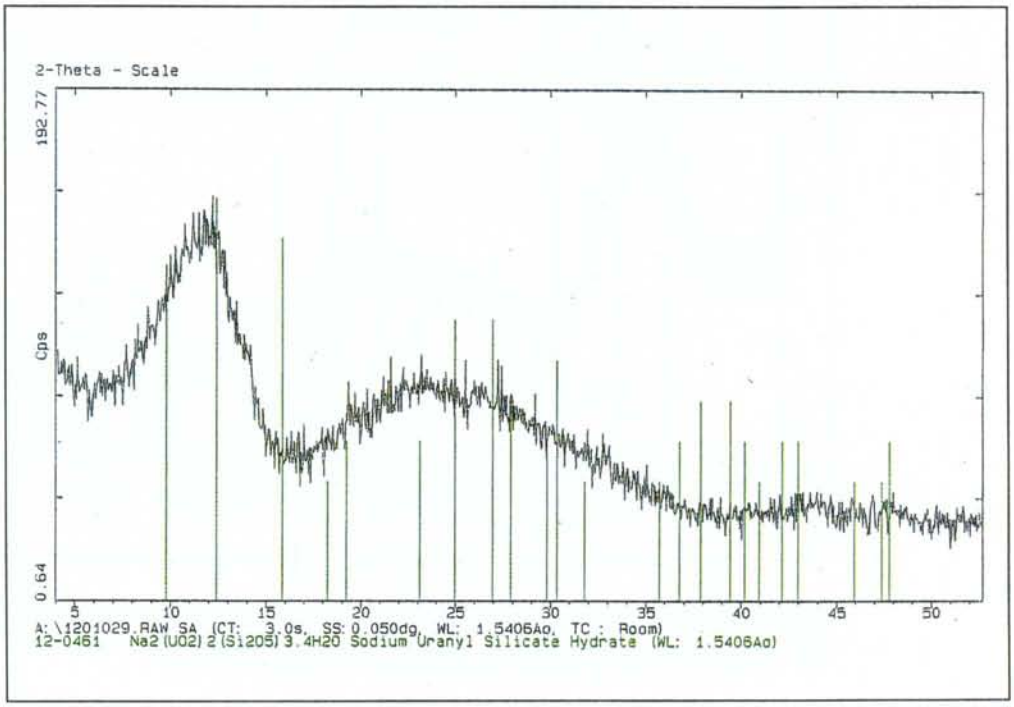

Figure 2-5. *X-ray powder-diffraction pattern of synthetic soddyite (batch A). Before the treatment to improve its crystallinity.*

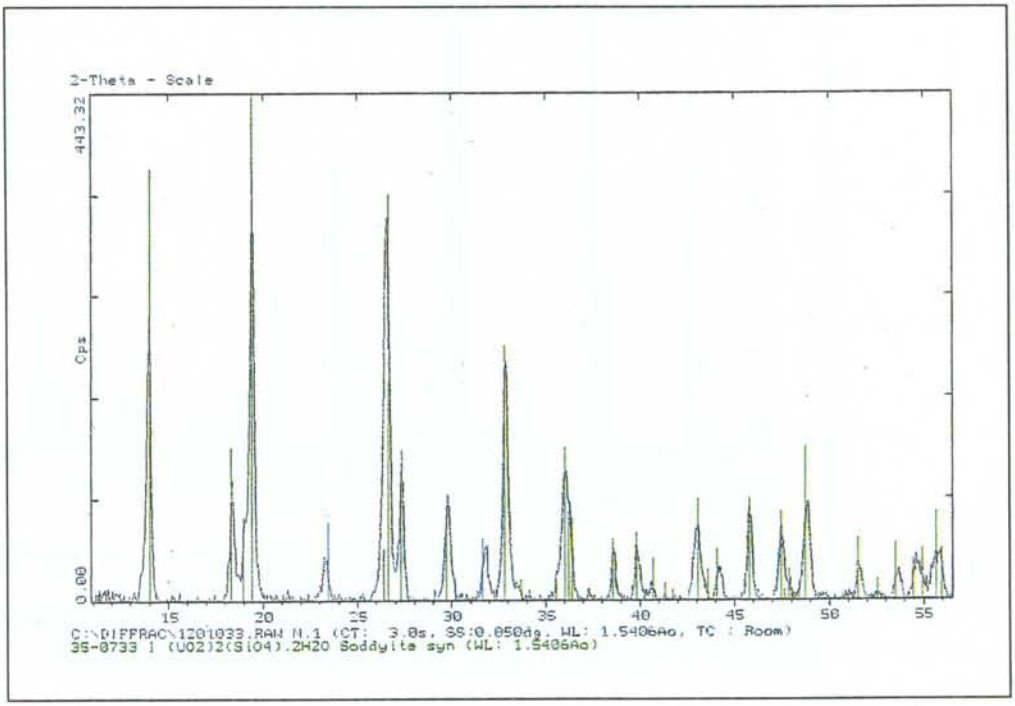

Figure 2-6. *X-ray powder-diffraction pattern of synthetic soddyite (batch A). After two weeks of treatment to improve its crystallinity.*

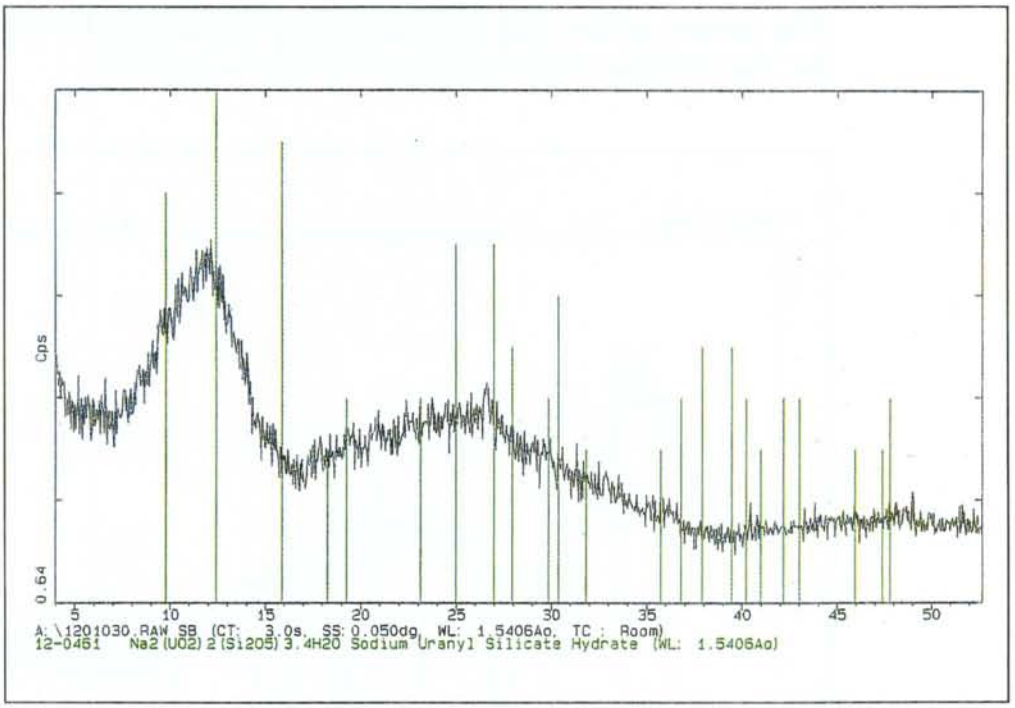

Figure 2-7. *X-ray powder-diffraction pattern of synthetic soddyite (batch B). Before the treatment to improve its crystallinity.*

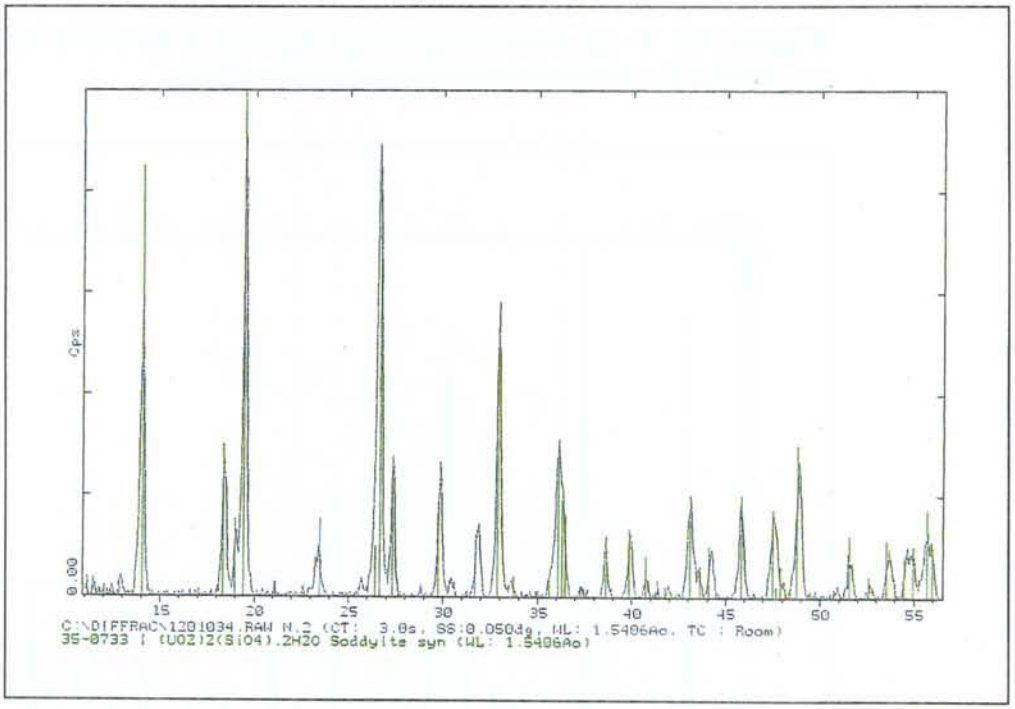

Figure 2-8. *X-ray powder-diffraction pattern of synthetic soddyite (batch B). After two weeks of treatment to improve its crystallinity.*

The uranophane synthesized from uranyl acetate did not show a significant increase of the crystal size after the treatment of the solid at 120°C for 18 days (Figures 2-9 and 2-10).

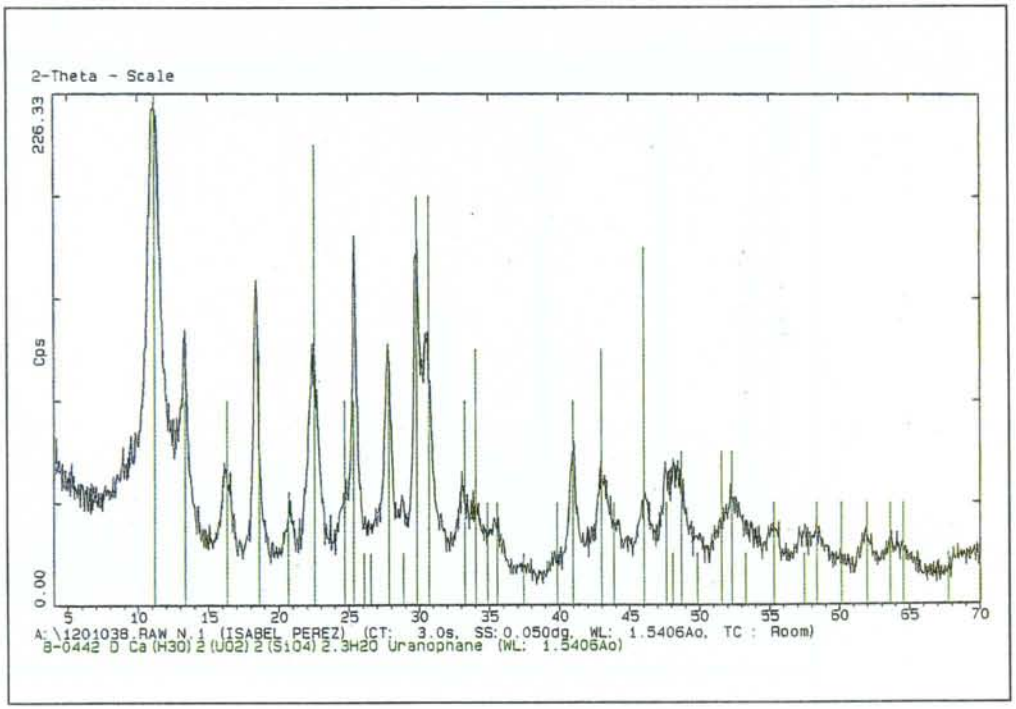

Figure 2-9. *X-ray powder-diffraction of synthetic uranophane (batch C). Before the treatment to improve its crystallinity.*

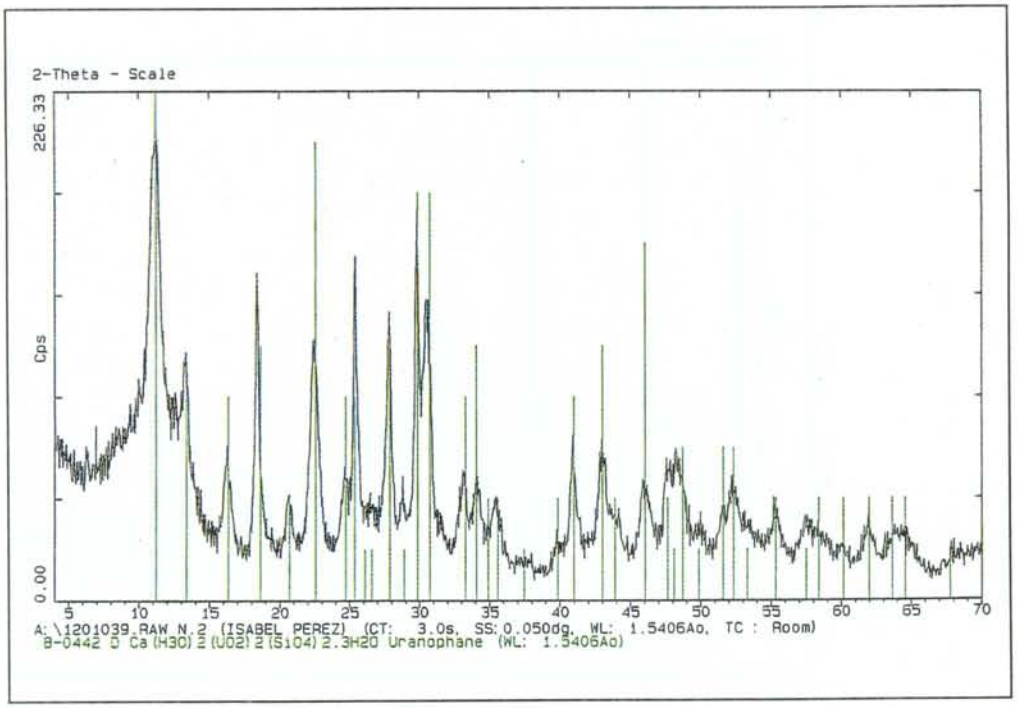

Figure 2-10. *X-ray powder-diffraction of synthetic uranophane (batch C). After 18 days of treatment to improve its crystallinity.*

As in the case of uranophane, the synthesis from uranyl acetate did not yield a crystalline solid (Figures 2-11 and 2-12).

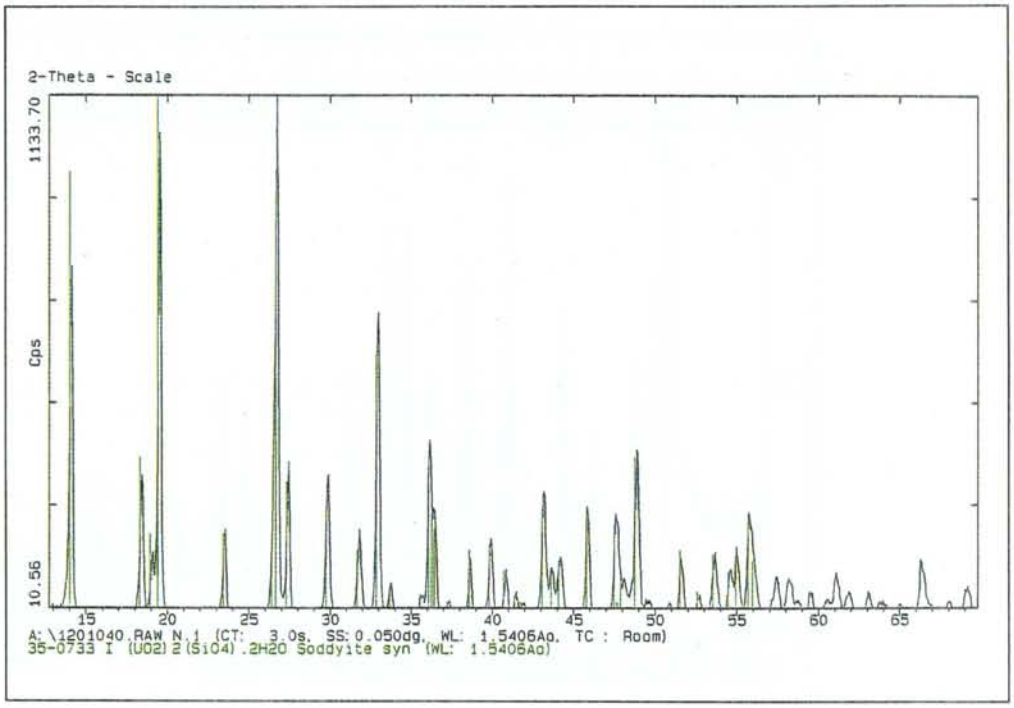

Figure 2-11. *X-ray powder-diffraction of synthetic soddyite (batch C). Before the treatment to improve its crystallinity.*

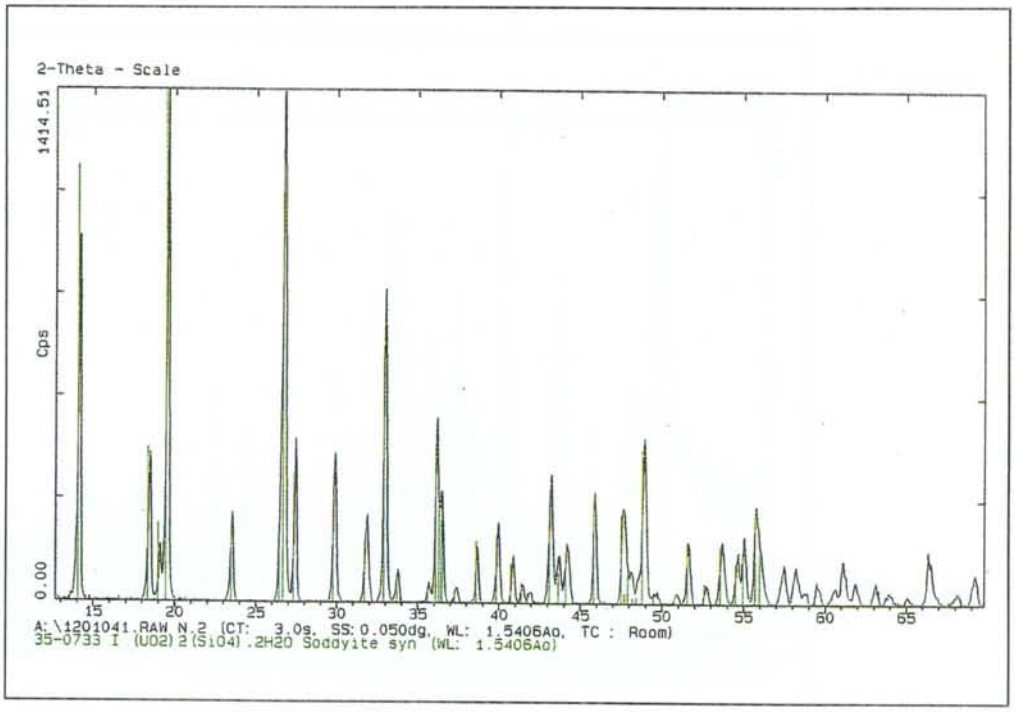

Figure 2-12. *X-ray powder-diffraction of synthetic soddyite (batch C). After four weeks of treatment to improve its crystallinity.*

2.2.2 FTIR

The FTIR absorbance spectra were carried out on a Nicolet 520 FT-IR system in the region from 4000 cm^{-1} to 400 cm^{-1}. Each sample was mixed with KBr, ground to a fine powder and pressed into a clear disk. Then, it was directly examined. A laser of He/Ne was used as reference to constantly calibrate the scale of frequency of the instrument. The results obtained for the different synthesized solid phases are presented in Figure 2-13.

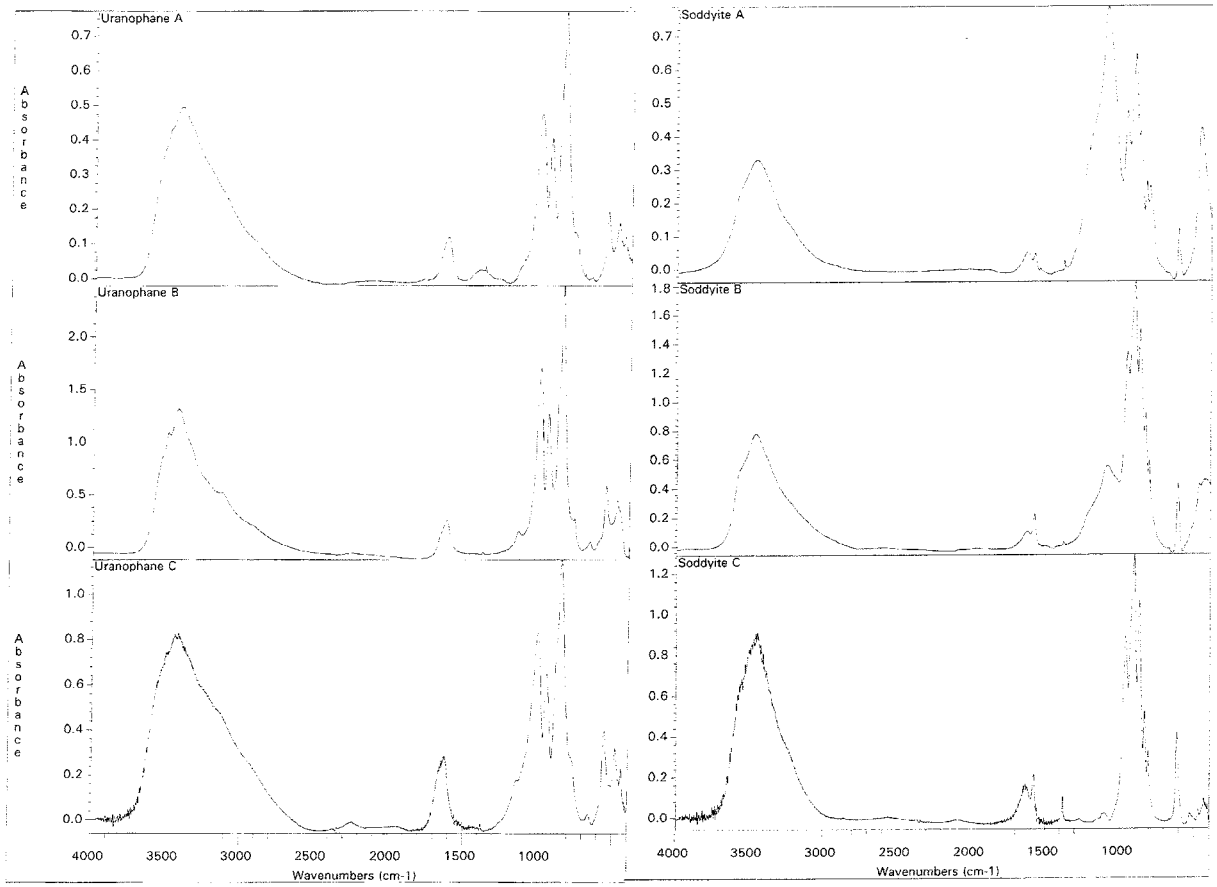

Figure 2-13. *FTIR spectra obtained for soddyite and uranophane*

The broad band in the region comprised between 3800 cm^{-1} and 3000 cm^{-1} corresponds to vibrational stretching modes of the water of hydration. A band centered at 1630 cm^{-1} corresponds to a symmetrical bending mode of water. The UO_2^{2+} group exhibits only one band at 1001 cm^{-1} (uranophane) and 962 cm^{-1} (soddyite) (Nakamoto, 1986). In the region from 950 cm^{-1} to 550 cm^{-1} the SiO_4^{-4} group exhibits three bands (Nakamoto, 1986). In the FTIR spectra of synthetic soddyite we can observe two bands (1097 cm^{-1} and 467 cm^{-1}) which are assigned to an amorphous silica (Nyquist and Kagel, 1971). These bands are not observed in the soddyite synthesized from uranyl acetate (Soddyite C).

2.2.3 SEM

Scanning Electron Microscopy (SEM) allows to visualize the surface of the sample. When it is combined with energy dispersive X-ray spectroscopic analysis (EDS) it provides information about the solid chemical composition. The analysis were performed by using a JEOL 6450, EDX-LINK-LZ5 system.

Two pictures corresponding to uranophane and soddyite, respectively, are presented below (Figures 2-14 and 2-15), where the formation of crystals of an homogeneous, though small, size is observed.

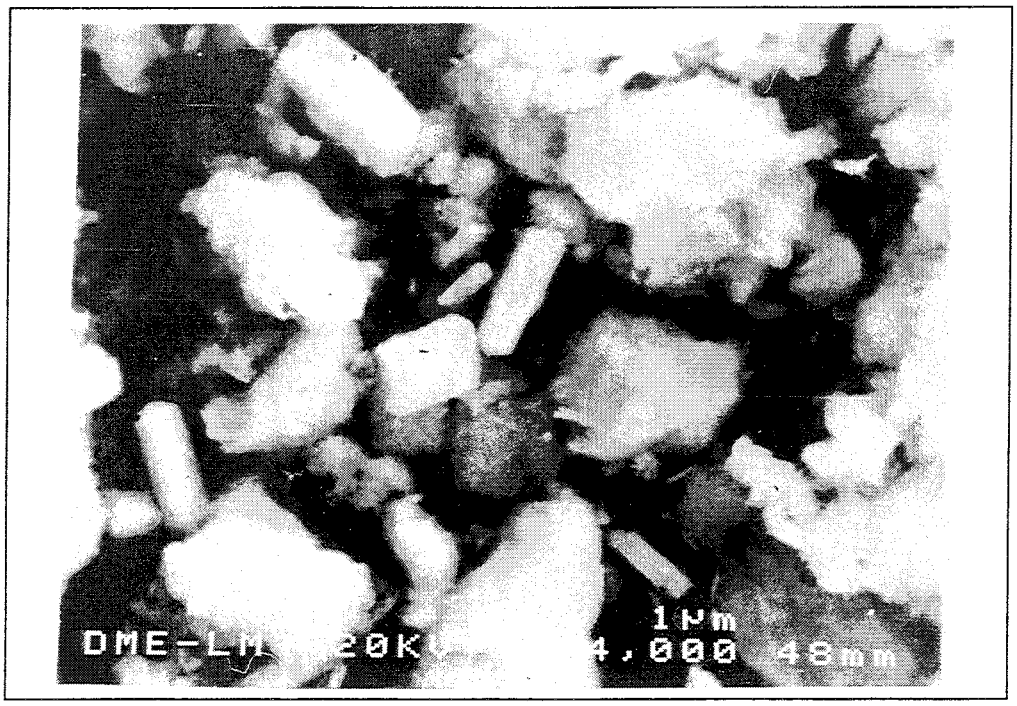

Figure 2-14. *SEM photomicrograph of uranophane.*

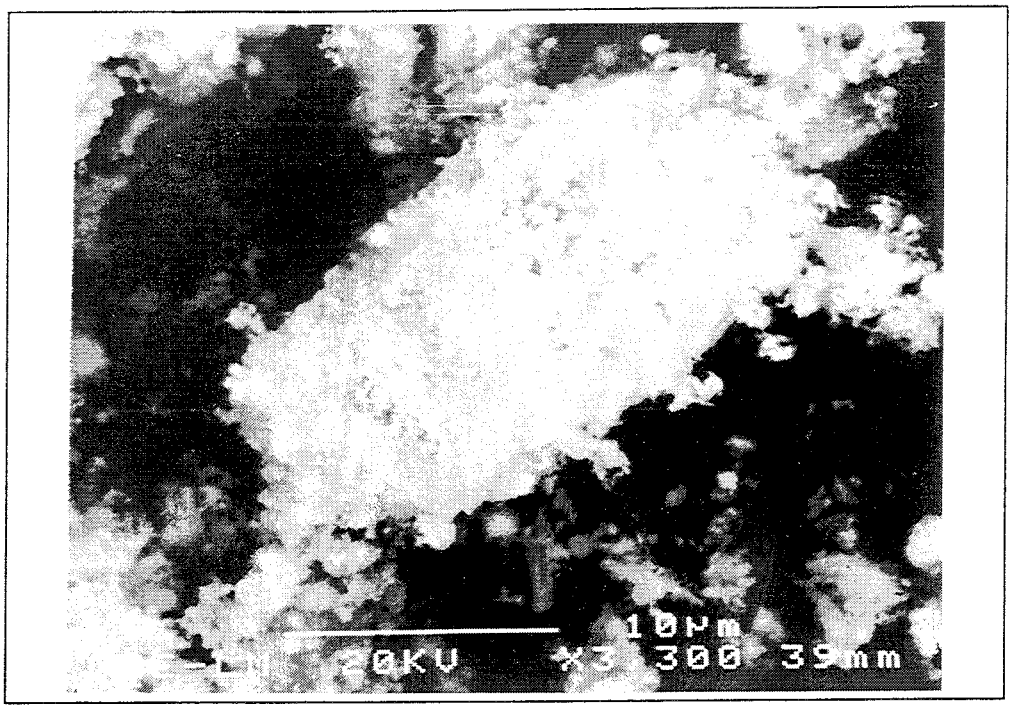

Figure 2-15. *SEM photomicrograph of soddyite.*

The SEM pictures of the synthesized uranophane (Figure 2-16) and soddyite (Figures 2-17) from uranyl acetate were taken after sputtering of the samples with ionized gold by vacuum until they were covered with a layer of 300 Å. The system used was a Balzers SDC004 Sputter Coater. This treatment allows to visualize the surface of the sample at greater magnifications.

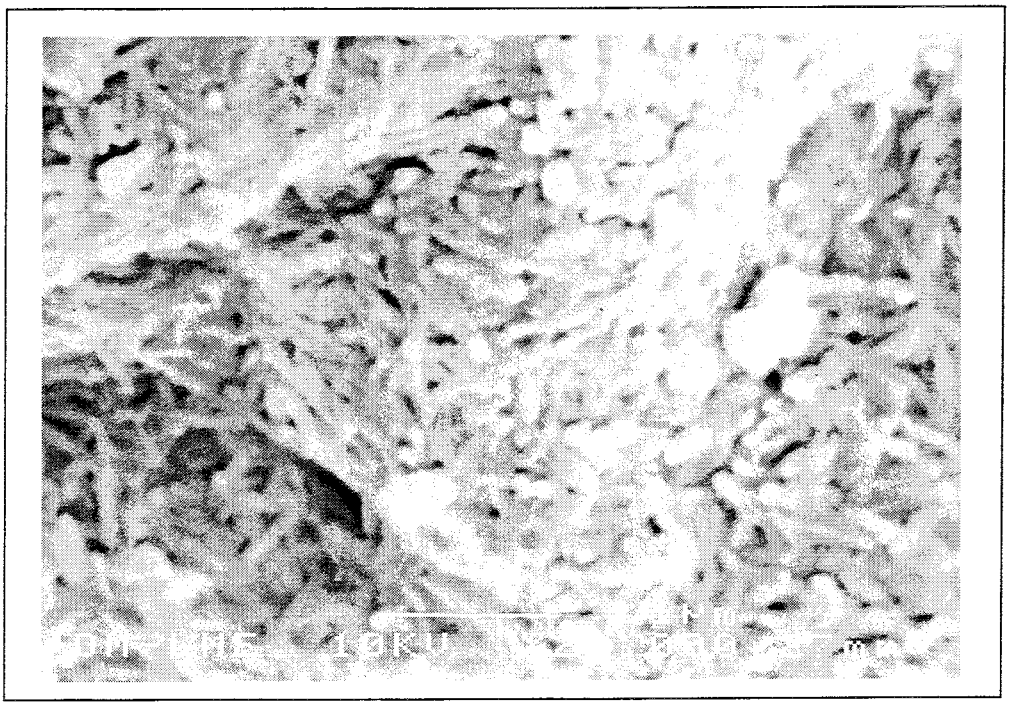

Figure 2-16. *SEM photomicrograph of uranophane*

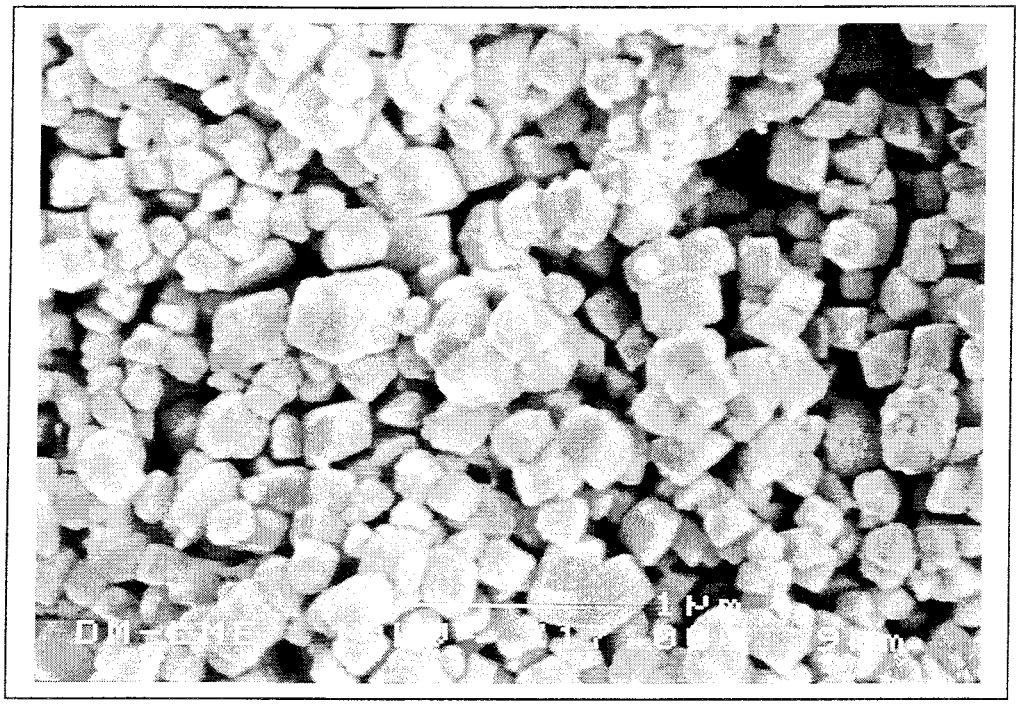

Figure 2-17. SEM photomicrograph of soddyite.

2.2.4 Surface area determination

Surface area is an important factor that affects the dissolution rate (Nyquist and Kagel, 1971). The BET gas adsorption method has become the most widely used standard procedure for the determination of the specific surface area of granulated and powdered solids or porous materials (Rothenberg et al., 1987).

The specific surface area for each solid was measured with a FLOWSORB II 2300 system of Micromeritics, determining the quantity of nitrogen gas adsorbed on the surface by measuring the thermal conductivity of the adsorbate gas. This adsorption takes place at or near the boiling point of the adsorbate gas. Under specific conditions, the area covered by each gas molecule is known within relatively narrow limits. The area of the sample is thus directly calculated from the number of adsorbed molecules, which is derived from the gas quantity at the prescribed conditions, and the area occupied by each molecule (Sing et al., 1985).

Previous to determining the specific surface area, a known weight of each sample was heated in an oven at 353 K for several hours in order to remove moisture and other adsorbed vapors.

The gas mixture employed was 30% N_2 and 70% He and the coolant used was liquid nitrogen.

The FLOWSORB is calibrated by injecting 1 ml of nitrogen gas through a septum and setting the instrument to value calculated at room temperature and atmospheric pressure for the surface area of nitrogen. This process must

be continued until there is no change in the area determined for repeated injections.

The specific surface area for a known amount of each solid phase was determined from repeated nitrogen adsorptions to the solid surface and their respective desorptions until the adsorption and desorption processes presented the same value.

The specific surface area obtained for all synthesized solid phases are shown in Table 2-1.

Table 2-1. Specific surface areas determined for the solids under study.

Solid phase	Specific Surface Area ($m^2 \cdot g^{-1}$)
Uranophane A	54.93 ± 0.12
Uranophane B	20.14 ± 0.14
Uranophane C	35.45 ± 0.52
Soddyite A	65.75 ± 0.09
Soddyite B	25.41 ± 0.19
Soddyite C	6.36 ± 0.29

2.3 DISSOLUTION EXPERIMENTS

2.3.1 Methodology

Solubility studies of the synthetic uranyl silicates were performed in two different ways in order to determine separately the influence of pH and $[HCO_3^-]$ on the kinetic and thermodynamic properties. All the studies were made at room temperature. An orbital stirrer was used to keep the solution homogeneously mixed as well as to minimize physical alterations of the solid phase.

The leaching solution compositions were selected trying to prevent the formation of secondary solid phases during the leaching of the samples. This selection was based in the so far available database for the two uranium silicates. All solutions were prepared with double distilled water. The water was collected from a Millipore filtration system.

The composition of the two leaching solutions was:

Uranophane experiments: 10^{-2} mol dm^{-3} $Ca(ClO_4)_2 \cdot 4H_2O$ and 10^{-3} mol dm^{-3} Na_2SiO_3. The ionic strength resultant was 0.033 mol dm^{-3}.

Soddyite experiments: 10^{-3} mol dm^{-3} Na_2SiO_3 and $7 \cdot 10^{-3}$ mol dm^{-3} $NaClO_4.H_2O$ in order to have an ionic strength of 0.01 mol dm^{-3}. The perchlorate was used in order to avoid complexation of uranium other than the one due to the presence of hydroxyl and carbonate.

To allow a relatively short saturation time, the solid surface/solution volume ratio was selected to be relatively high. This implied the use of a small

volume of solution. The initial volume of the test solution was 100 ml. The weight of solid used ranged from 0.25 g (soddyite) to 0.50 g (uranophane).

i) Carbonate free experiments

These series of experiments were carried out in the following way. The leaching solutions were prepared carbonate free and nitrogen was continuously bubbled throughout the experimental time. For each experiment a known mass of solid uranyl silicate was transferred to a Teflon vessel containing 100 ml of the test solution. The pH of the leaching solution was previously adjusted to the required value by using either $HClO_4$ or carbonate-free NaOH solution. The test solution was prepared slightly more basic than the desired pH to compensate the pH drop when uranyl silicate was added to the solution. The pH of the solutions was measured by a combined glass electrode calibrated every two weeks with pH=7 and pH=4 buffer solutions to correct for any pH drift.

The dissolution of these samples was followed as a function of time. We assumed that equilibrium was reached when aqueous uranium concentration and pH reading remained constant for several days (see figures below). After the equilibrium state was reached, the solution was completely replaced by a fresh one, with the pH previously set to the desired new value. This systematic allows kinetic determinations for the different pH values studied.

In addition, two experiments were performed in distilled water to check the possibility of being the solution composition the responsible of the precipitation observed. However, in these cases (pH 7.2 and 11.7) precipitation was also observed.

ii) Experiments in bicarbonate solution

Sodium bicarbonate was used in the test solution as a first approximation to granitic groundwater composition, where carbonate is found to be one of the most important complexing agent.

The experiments were performed without nitrogen, in methacrillate vessels. Different bicarbonate concentrations were used in order to determine the influence of this anion on the dissolution of both uranophane and soddyite.

The pH values of the experiments were buffered by the carbonate content of the test solution in equilibrium with the carbon dioxide of the air.

The dissolution of these samples was again followed as a function of time. When equilibrium was reached, the solution was completely replaced by a fresh one, with the preset bicarbonate concentration.

It is important to note here the fact that uranophane showed precipitation of secondary solid phases even in the presence of bicarbonate. For this reason, the experiments were performed in distilled water with addition of bicarbonate to reach the corresponding concentration. In these cases, no precipitation took place, and these are the results that will be discussed here.

2.3.2 Analytical methods

Uranium concentrations in solution were measured for all the experiments, for each sample taken.

During the first hour of the experiments as many samples as possible were taken (one aliquot of 0.5 or 1 ml each) in order to follow the very initial kinetic of the reaction. After this time, three aliquots of 0.5 or 1 ml were taken for each sampling point, at longer intervals of time.

Samples were immediately filtered through Millipore filters of 0.20 μm nominal pore size to ensure that only dissolved uranium contributed to the analysis. When it was necessary to store the solutions for some time before analysis, they were acidified with a small volume of concentrated HNO_3 to prevent uranium precipitation and/or adsorption.

The determination of the uranium concentration was made using a Scintrex UA-3 laser fluorescence analyzer. This technique is based on the fluorescence of an uranyl complex formed by addition of an inorganic complexing reagent (FLURAN) that converts the various uranyl species present in the solution into a single form that has a high luminescent yield.

Under ultraviolet excitation at a wavelength of 337 nm which is provided by a small nitrogen laser, uranyl salts emit a green luminescence that can be measured quantitatively by a suitable photodetector. The values obtained are compared with an uranyl nitrate standard solution.

Analysis with a sensitivity better than 0.05 ppb of uranium can be made without pre-concentration or treatment of the sample even in the presence of some potentially interfering species (de Pablo et al., 1992).

3 RESULTS

3.1 SODDYITE DISSOLUTION

3.1.1 Carbonate free leaching solutions

In the experiments performed using test solutions free of carbonate, an erratic behavior was observed among the experiments (Figures 3-1 and 3-2). In some cases, precipitation of uranium occurred (Figure 3-1).

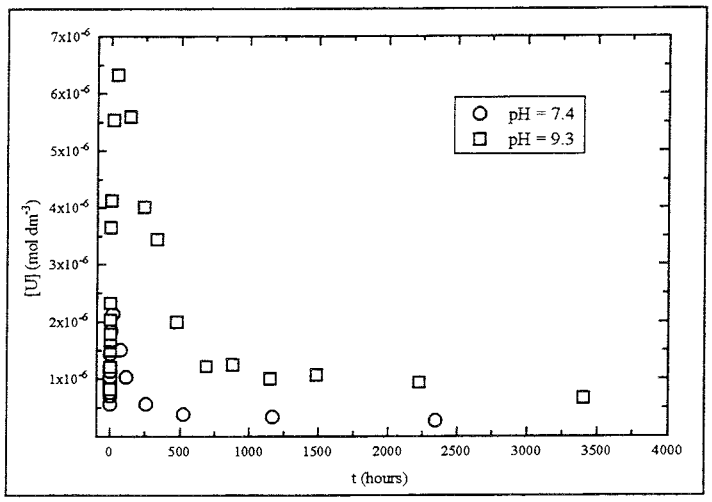

Figure 3-1. *Total dissolved uranium concentration as a function of time for the dissolution of soddyite in bicarbonate free medium at pH 7.4 and 9.3*

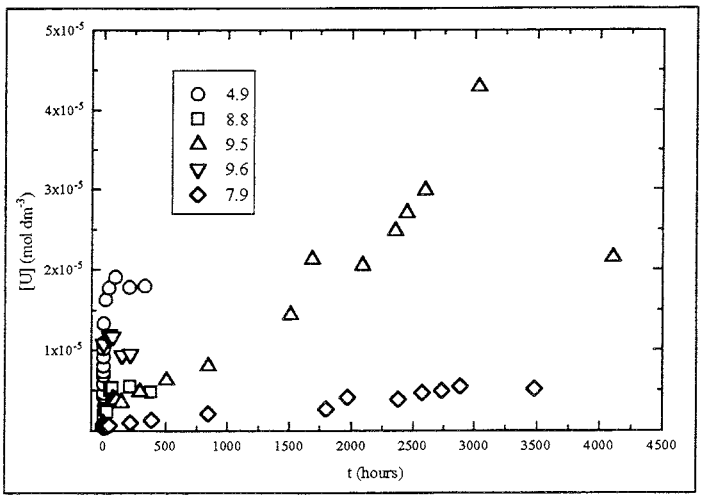

Figure 3-2. *Total dissolved uranium concentration as a function of time for the dissolution of soddyite in bicarbonate free medium at pH 4.9, 7.9, 8.8, 9.5 and 9.6.*

For the rest of the experiments, although precipitation of uranium was not evident, no clear equilibrium state was reached, even for experiments performed for about 4500 hours (Figure 3-2).

3.1.2 Carbonated leaching solutions

Table 3-1 summarizes the uranium concentration at steady-state for each bicarbonate concentration in solution and the pH values reached. In some cases (1, 2 and 5 mM of total sodium bicarbonate), duplicate experiments were performed, which showed reproducibility of both dissolution rates and uranium saturation levels.

Table 3-1. Experimental values obtained at the end of the different experiments performed with soddyite, including the total bicarbonate concentrations, the pH measured at the end of the experiment and the average total uranium concentration in solution, in mol dm^{-3}.

$[HCO_3^-]_{tot}$ (mol dm^{-3})	pH	log $[U]_{tot}$
$1.0 \cdot 10^{-3}$	8.7 ± 0.3	-4.29 ± 0.05
$1.0 \cdot 10^{-3}$	8.7 ± 0.2	-4.25 ± 0.01
$2.0 \cdot 10^{-3}$	8.5 ± 0.2	-4.08 ± 0.01
$2.0 \cdot 10^{-3}$	8.8 ± 0.3	-4.05 ± 0.07
$5.0 \cdot 10^{-3}$	8.72 ± 0.03	-3.45 ± 0.04
$5.0 \cdot 10^{-3}$	8.65 ± 0.04	-3.54 ± 0.03
$8.0 \cdot 10^{-3}$	9.11 ± 0.09	-3.07 ± 0.01
$1.0 \cdot 10^{-2}$	8.54 ± 0.07	-2.99 ± 0.03
$1.5 \cdot 10^{-2}$	8.6 ± 0.2	-2.72 ± 0.03
$2.0 \cdot 10^{-2}$	8.8 ± 0.1	-2.65 ± 0.01

The behavior of the system showed a fast initial increase of the uranium in solution before the final steady state was reached. The general trend of the total measured uranium concentration in solution is shown in Figure 3-3 (the results are presented in three different figures to allow a better scaling of the experimental data presented).

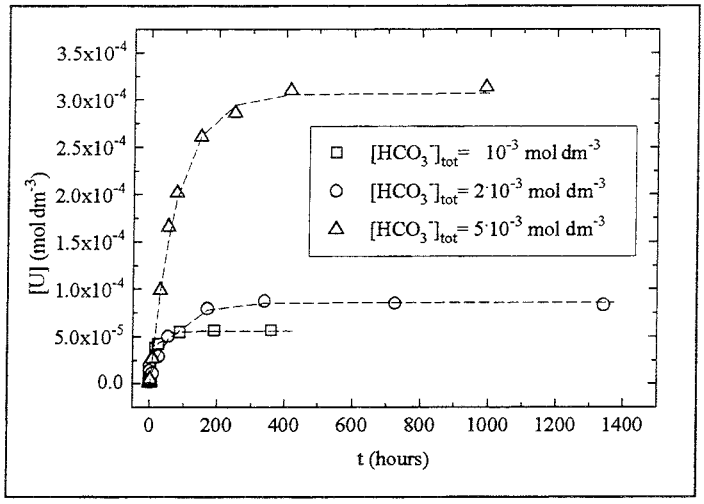

(a)

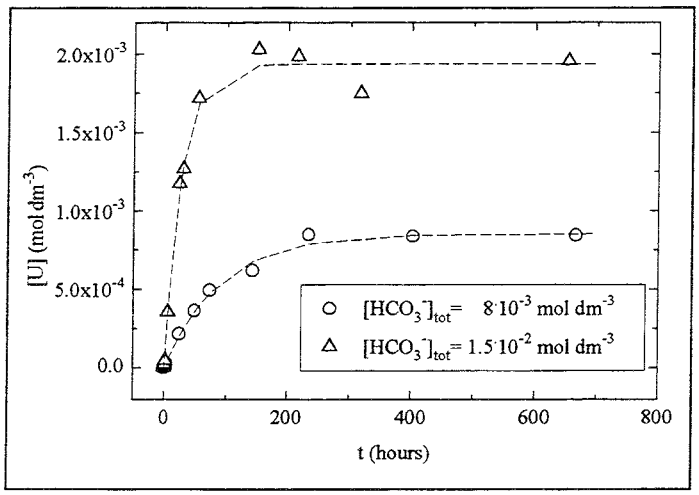

(b)

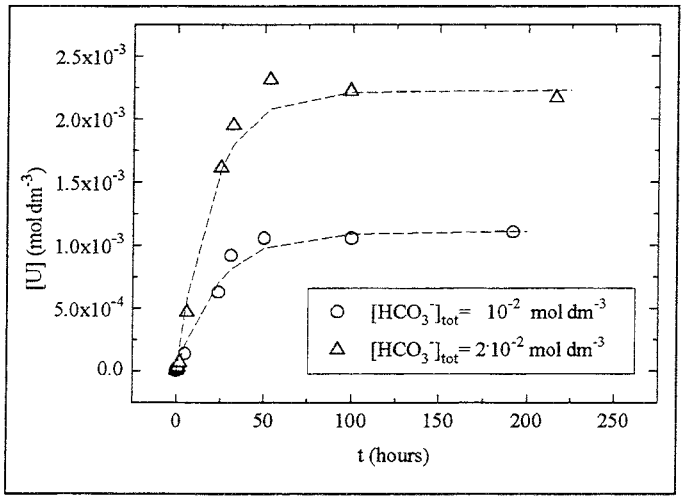

(c)

Figure 3-3. *Total measured uranium in solution as a function of time for different total bicarbonate concentrations. Dashed lines correspond to the dissolution model calculated using equation (5) (see Discussion section).*

3.2 URANOPHANE DISSOLUTION

3.2.1 Carbonate free leaching solutions

The results obtained in the uranophane leaching experiments performed using bicarbonate free test solutions can be classified in two different groups. On one side, the experiments performed at acidic pH values (4.7, 5.0 and 5.1) show a dissolution trend leading to the saturation of the aqueous solution (Figure 3-4). In addition, the two experiments performed at pH values 4.7 and 5.0, show very similar results, as it could be expected from the slight difference in experimental conditions. However, the experiment performed at pH 5.1 shows an initial precipitation though at longer periods of time it evolved again to a dissolution trend, but no equilibrium was achieved in this case during the experimental time (1000 hours). On the other hand, there is a second group of experiments (Figure 3-5) corresponding to the assays carried out at neutral to alkaline pH values (7.8, 8.7, 9.1, 9.4, 9.6 and 9.7). In all these experiences, an initial dissolution took place, although a subsequent precipitation was observed at very early stages (approximately after two days). XPD observations of the final solid phase showed the presence of a precipitated U(VI)-silicate phase different of uranophane, though not clearly identified (Figure 3-6).

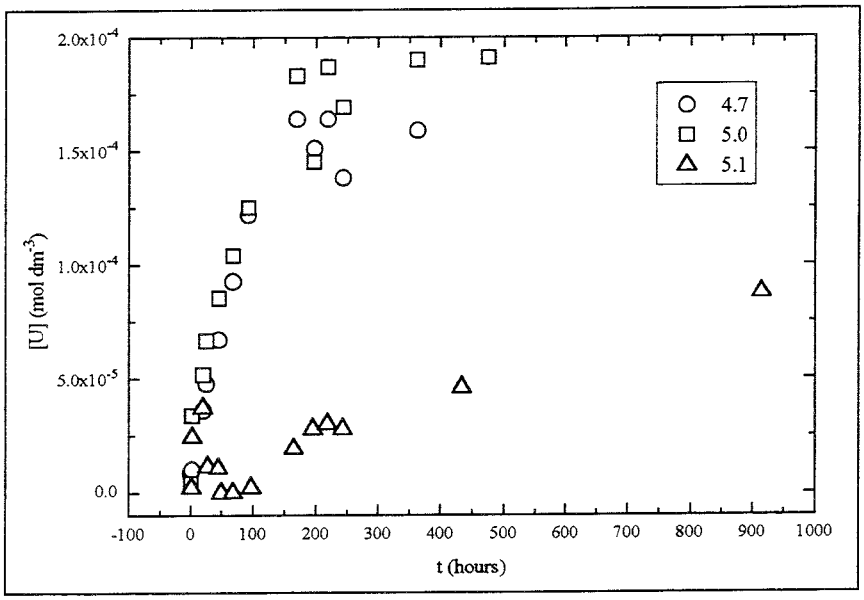

Figure 3-4. *Leaching experiments for uranophane in absence of bicarbonate and for acidic pH values.*

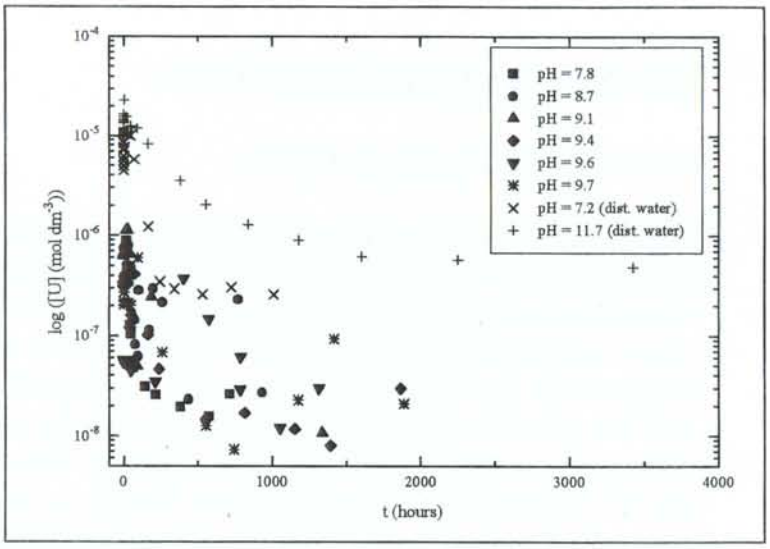

Figure 3-5. *Logarithm of the total uranium in solution for the leaching experiments of uranophane in absence of bicarbonate and for neutral to alkaline pH values. The two experiments performed in distilled water are also included.*

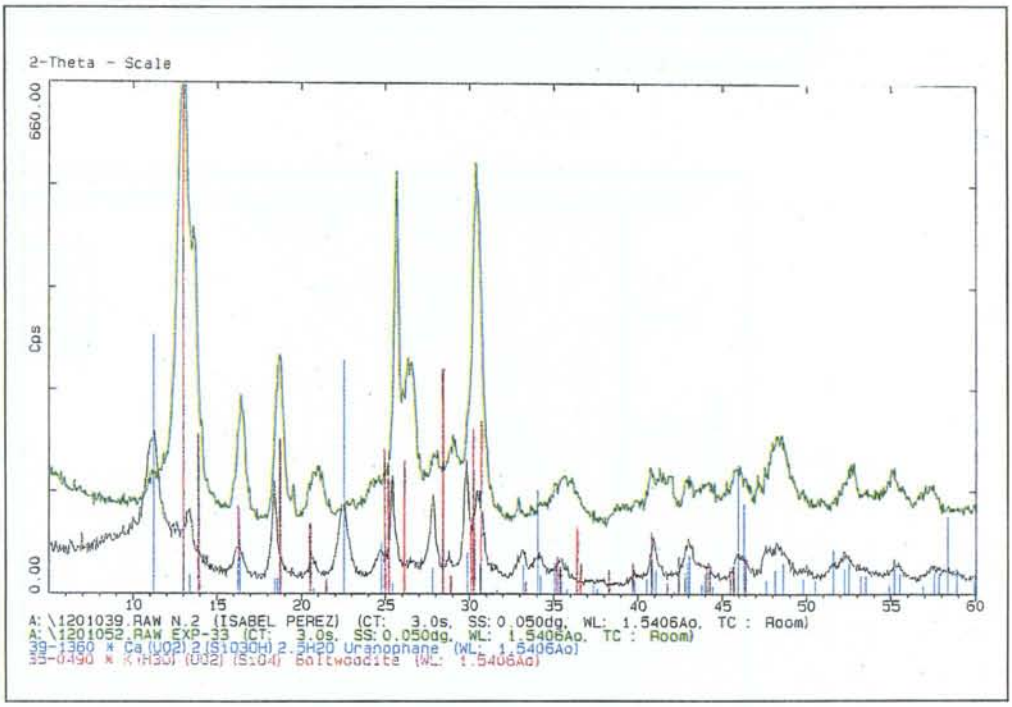

Figure 3-6. *XPD diffractogram of the solid phase obtained at the end of a bicarbonate free dissolution experiment performed at alkaline pH (11.73).*

3.2.2 Carbonated leaching solutions

Table 3-2 summarizes the uranium concentration at steady-state for each bicarbonate concentration in solution and the pH values reached. In some cases (1, 5, 15 and 20 mM of total sodium bicarbonate), duplicate

experiments were performed. We remind here that these experiments were performed in distilled water with the corresponding bicarbonate concentration.

Table 3-2. Experimental values obtained at the end of the different experiments performed with uranophane, including the total bicarbonate concentrations, the pH measured at the end of the experiment and the average total uranium concentration in solution, in mol dm^{-3}.

$[HCO_3^-]_{tot}$ (mol dm^{-3})	pH	log $[U]_{tot}$
$1.0 \cdot 10^{-3}$	8.0 ± 0.1	-4.32 ± 0.02
$1.0 \cdot 10^{-3}$	8.1 ± 0.2	-4.40 ± 0.02
$2.0 \cdot 10^{-3}$	8.52 ± 0.01	-4.40 ± 0.01
$5.0 \cdot 10^{-3}$	8.68 ± 0.03	-4.00 ± 0.02
$5.0 \cdot 10^{-3}$	8.64 ± 0.01	-3.75 ± 0.01
$5.0 \cdot 10^{-3}$	8.65 ± 0.02	-3.81 ± 0.01
$8.0 \cdot 10^{-3}$	8.9 ± 0.1	-3.76 ± 0.02
$1.0 \cdot 10^{-2}$	9.1 ± 0.1	-3.49 ± 0.05
$1.5 \cdot 10^{-2}$	8.75 ± 0.04	-3.16 ± 0.01
$1.0 \cdot 10^{-2}$	8.82 ± 0.05	-3.20 ± 0.01
$2.0 \cdot 10^{-2}$	9.37 ± 0.03	-3.22 ± 0.01
$2.0 \cdot 10^{-2}$	9.0 ± 0.1	-3.12 ± 0.02

The behavior of the system showed, as in the case for soddyite, a fast initial increase of the uranium in solution before a final steady state was reached. The general trend of the total measured uranium concentration in solution is shown in Figure 3-7 (again, the results are presented in different figures to allow a better scaling of the experimental data presented).

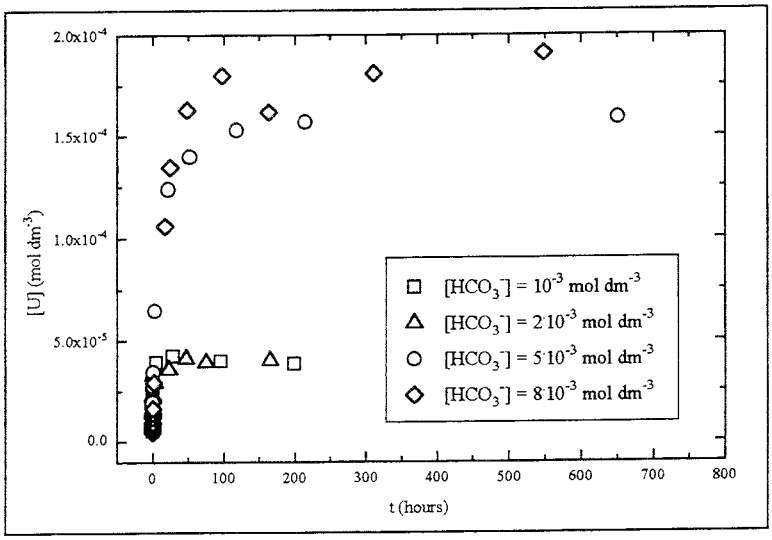

(a)

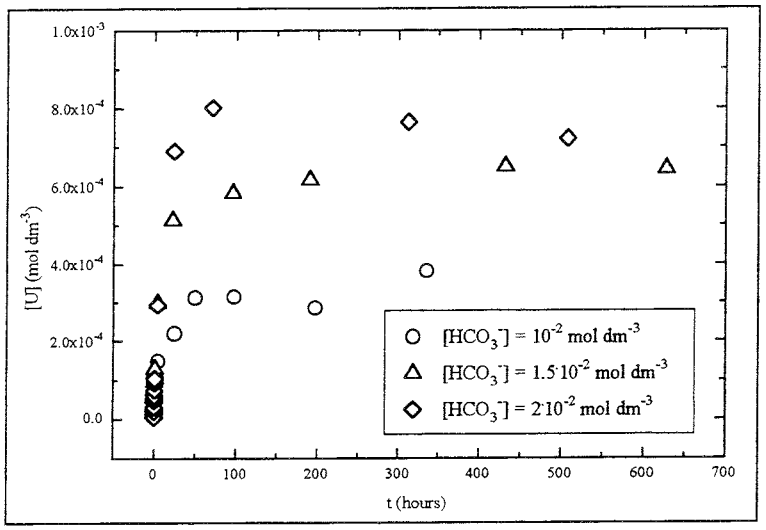

(b)

Figure 3-7. *Total measured uranium in solution as a function of time for different total bicarbonate concentrations.*

4 DISCUSSION

4.1 SODDYITE

4.1.1 Thermodynamics

Due to the erratic behavior observed for the uranium concentrations in the experiments performed in the absence of bicarbonate, which is attributed to the formation of a secondary solid phase, the discussion of the results will concentrate on the results obtained in the experiments performed in the presence of sodium bicarbonate in the test solution.

The aqueous uranium speciation at steady-state was calculated using the HARPHRQ code, and using for uranium the SKBU database (Bruno and Puigdomènech, 1989). These calculations showed that the $UO_2(CO_3)_3^{4-}$ complex is the dominant aqueous species (more than 90%) at bicarbonate concentrations larger than 5 mM. Hence, the dissolution reaction of soddyite can be written as:

$$(UO_2)_2SiO_4.2H_2O + 6HCO_3^- \Leftrightarrow 2UO_2(CO_3)_3^{4-} + H_4SiO_4 + 2H^+ + 2H_2O \quad \textbf{5-1}$$

and the corresponding equilibrium constant:

$$K = a_{\text{uranyl complex}}^{2} \cdot a_{\text{silicon}} \cdot a_{\text{proton}}^{2} \cdot a_{\text{bicarbonate}}^{-6} \quad \textbf{5-2}$$

From the total bicarbonate concentration, the silicon in solution (calculated as the initial silicon concentration in solution plus the amount due to dissolution, assuming congruent release with uranium) and the experimental pH, we calculated the equilibrium constant for each experiment using again the HARPHRQ code. These constants were subsequently corrected to zero ionic strength by using the specific ion interaction theory (SIT) (Grenthe et al., 1992). Finally, from the equilibrium constants obtained, K_{S0} values corresponding to dissolution reaction (5-3) were calculated:

$$(UO_2)_2SiO_4.2H_2O + 4H^+ \Leftrightarrow 2UO_2^{+2} + H_4SiO_4 + 2H_2O \quad \textbf{5-3}$$

Table 4-1 lists values of the ionic strengths of the reaction media obtained from the HARPHRQ code as well as the values of both log $K_{(I=0)}$ and log K_{S0} calculated for each experiment.

It can be seen that, at low bicarbonate concentrations, where other complexed uranyl species play an important role, the log K_{S0} values obtained clearly differ from those obtained at higher bicarbonate concentrations. Therefore, only the values of log K_{S0} obtained at bicarbonate concentrations greater than 2 mM were averaged to get the final proposed value of log K_{S0}:

Table 4-1. Calculated equilibrium constant at infinite dilution and the solubility product for each bicarbonate concentration.

$[HCO_3^-]_{tot}$ (mol dm^{-3})	Ionic strength	log K (I_m=0)	log K_{S0}
$1.0 \cdot 10^{-3}$	0.0087	-12.48	6.30
$1.0 \cdot 10^{-3}$	0.0087	-12.42	6.36
$2.0 \cdot 10^{-3}$	0.0095	-13.15	5.63
$2.0 \cdot 10^{-3}$	0.0096	-13.37	5.41
$5.0 \cdot 10^{-3}$	0.0129	**-14.18**	**4.60**
$5.0 \cdot 10^{-3}$	0.0124	**-14.36**	**4.42**
$8.0 \cdot 10^{-3}$	0.0182	**-14.98**	**3.80**
$1.0 \cdot 10^{-2}$	0.0196	**-14.54**	**4.24**
$1.5 \cdot 10^{-2}$	0.0280	**-15.01**	**3.77**
$2.0 \cdot 10^{-2}$	0.0333	**-16.20**	**2.58**

In Figure 4-1, we show a comparison of the experimental uranium concentrations and the calculated uranium concentrations obtained by using different values of log K_{S0}. These values include the log K_{S0} calculated for each experiment, as presented in Table 4-1, as well as the average value proposed in this work, and, finally the value reported by Nguyen et al. (1992) (log K_{S0}=5.74). The solubility constant recently published in Moll et al. (1996) (log K^0_{s0}=6.15) is not included because it would give a model very similar than the one obtained for log K_{s0}=5.74. The model presented in Figure 4-1 obtained using a log K_{s0}=5.74, clearly gives in all cases higher calculated than experimental uranium concentrations.

The difference on the solubility constant proposed in this work and the previously published (Nguyen et al., 1992; Moll et al., 1996) is attributed to the differences in the experimental methodology and conditions. Nguyen et al. (1992) and Moll et al. (1996) used a single experimental data (at pH approximately 3 in both studies) to extract the solubility product of soddyite, while in our case, a set of data was fitted to calculate K_{S0}. In addition, we used bicarbonate in our test solution. This anion constitutes an important complexing agent for aqueous U(VI), which results in the stabilization of uranium in solution, reducing the possibility of formation of secondary solid phases. Such a secondary solid phase formation has been observed in our laboratory in some experiments performed at neutral to alkaline pH values without bicarbonate in the solution.

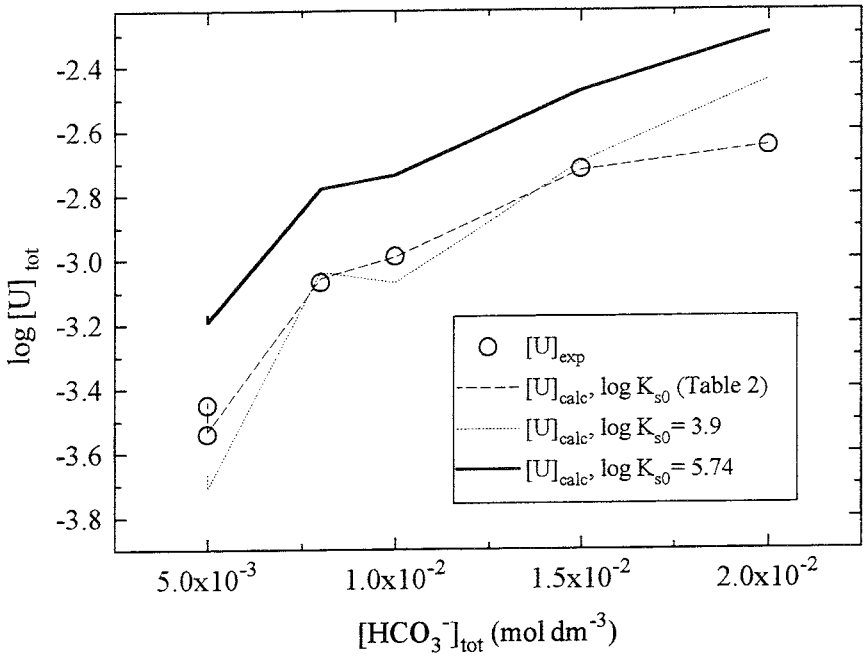

Figure 4-1. *Experimental solubilities obtained as a function of total bicarbonate concentration as well as calculated solubilities obtained by using different K_{S0} (see legend).*

On the other hand, the solubility product obtained in this work can also be compared with the value obtained in experiments where a natural uranium phase was used (Casas et al., 1994). In that case, a log K_{S0} of 3.0±2.9 was determined.

Finally, there is still another solubility product of soddyite found in the literature with a value of log K_{s0} = 0.44. It is included in the HATCHES database used by the HARPHRQ geochemical code and that was extracted from a former EQ3/6 database. This value has not been considered in the discussion because the large inconsistency shown with the constants presented above as well as to the value presented in this work.

4.1.2 Kinetics

The simplest method used for determining the dissolution rate was the least-squares regression of the initial linear uranium concentrations obtained as a function of time.

The second method used was as follows. The principle of detailed balancing (Lasaga et al., 1983) was applied to reaction (1). Hence, the net rate of the reaction can be expressed as:

$$r = d[U]/dt = k_1[HCO_3^-]^6 - k_{-1}[UO_2(CO_3)_3^{4-}]^2\,[H_4SiO_4]\,[H^+]^2 \qquad \textbf{5-5}$$

In order to readily solve this equation some approximations were made. First of all, both bicarbonate concentration and pH have been considered to

remain constant through the experimental time. This assumption is considered to be reasonable as shown by the experimental measurements. In addition, the silicon released in the dissolution reaction was considered not significant compared to the initial concentration of this element in solution. Hence, a constant silicon concentration of 10^{-3} mol dm^{-3} was used in the modeling exercise. Calculations performed with the HARPHRQ code assuming congruent U-Si dissolution have shown that this approximation can be considered reasonable for most of the experiments performed.

Equation (5-5) was integrated and fitted to the experimental data. Both forward (k_1) and reverse (k_{-1}) rate constants were determined from the best fit obtained for each experiment. These fittings correspond to the dashed lines shown in Figure 3-3. As a test of the results obtained, we calculated the equilibrium constant from these rate constants as:

$$K_{eq} = k_1/k_{-1} \qquad \textbf{5-6}$$

From these equilibrium constants, corresponding to reaction (5-1), we calculated the solubility products corresponding to reaction (5-3). We obtained an average value of 4.3±0.6, which is in agreement with the solubility constant calculated from the equilibrium data in the preceding section, 3.9±0.7. This result gives confidence to the approximations made in the modeling process.

Finally, the experimental results were also modeled by using the EQ3/6 code package. This code uses the following rate equation:

$$R_{diss} = k_{diss} (1-10^{SI}) \qquad \textbf{5-7}$$

By comparing equations (5-7) and (5-5), we obtain:

$$k_{diss} = k_1 [HCO_3^-]^6 \qquad \textbf{5-8}$$

The comparison between the results obtained from the last two methods are shown in Table 4-2. Only the values that gave the best agreement between the two models are presented.

Hence, the following average dissolution rate of soddyite is proposed:

$$r_{diss} = 6.8\ (\pm 4.4)\ 10^{-10}\ \text{mol}\ m^{-2}\ s^{-1} \qquad \textbf{5-9}$$

No clear dependence neither on the proton nor on the bicarbonate concentrations was observed.

Table 4-2. Comparison of the results obtained by applying the principle of detailed balancing to reaction (5-1) and by using the EQ3/6 program.

$[HCO_3^-]_{tot}$ (mol dm^{-3})	k_{diss} (EQ3/6) (mol m^{-2} s^{-1})	$k_1[HCO_3^-]^6$ (mol m^{-2} s^{-1})
$8.0 \cdot 10^{-3}$	$1.23 \cdot 10^{-10}$	$1.39 \cdot 10^{-10}$
$1.0 \cdot 10^{-2}$	$8.23 \cdot 10^{-10}$	$5.29 \cdot 10^{-10}$
$1.5 \cdot 10^{-2}$	$1.23 \cdot 10^{-9}$	$4.22 \cdot 10^{-10}$
$2.0 \cdot 10^{-2}$	$1.23 \cdot 10^{-9}$	$9.26 \cdot 10^{-10}$

4.2 URANOPHANE

4.2.1 Thermodynamics

In this section we have only considered the results obtained in the experiments performed with bicarbonate in the test solutions. As it was the case for soddyite, the reason is the clear secondary phase formation observed in the experiments performed in the absence of bicarbonate.

The dissolution reaction of uranophane can be written as:

$$Ca(UO_2)_2(SiO_4)_2 3H_2O + 6H^+ \Leftrightarrow Ca^{+2} + 2UO_2^{+2} + 2\,H_4SiO_4 + 5H_2O \qquad \textbf{5-10}$$

Taking into account the low ionic strength of the test solutions, the solubility product is defined as:

$$K_{s0} = (a_{calcium})^2 \cdot (a_{uranyl})^2 \cdot (a_{silicon})^2 \cdot (a_{proton})^{-6} \qquad \textbf{5-11}$$

On the other hand, in the presence of relatively large bicarbonate concentration (i.e., larger than 5 mM), the dissolution reaction can be written as:

$$Ca(UO_2)_2(SiO_4)_2 3H_2O + 6HCO_3^- \Leftrightarrow Ca^{+2} + 2UO_2(CO_3)_3^{-4} + 2\,H_4SiO_4 + 5H_2O \qquad \textbf{5-12}$$

with an equilibrium constant defined as:

$$K = (a_{calcium})^2 \cdot (a_{uranyl\ complex})^2 \cdot (a_{silicon})^2 \cdot (a_{bicarbonate})^{-6} \qquad \textbf{5-13}$$

Following the same methodology already explained for soddyite, we calculated the value of K (eq. 5-13) and from it we recalculated the solubility product for uranophane (eq. 5-11), corrected to the zero ionic strength standard state, with the results presented in Table 4-3.

Table 4-3. Calculated equilibrium constant at infinite dilution and the solubility product of uranophane for each bicarbonate concentration.

$[HCO_3^-]_{tot}$ (mol dm^{-3})	Ionic strength	log K (I_m=0)	log K_{s0}
$1.0 \cdot 10^{-3}$	0.0011	-6.04	12.74
$1.0 \cdot 10^{-3}$	0.0011	-5.84	12.94
$2.0 \cdot 10^{-3}$	0.0023	-6.96	11.82
$5.0 \cdot 10^{-3}$	0.0059	**-7.47**	**11.31**
$5.0 \cdot 10^{-3}$	0.0064	**-6.10**	**12.68**
$5.0 \cdot 10^{-3}$	0.0062	**-6.50**	**12.28**
$8.0 \cdot 10^{-3}$	0.0097	**-7.73**	**11.05**
$1.0 \cdot 10^{-2}$	0.0131	**-7.04**	**11.74**
$1.5 \cdot 10^{-2}$	0.0206	**-6.70**	**12.08**
$1.5 \cdot 10^{-2}$	0.0203	**-6.82**	**11.96**
$2.0 \cdot 10^{-2}$	0.0278	**-8.03**	**10.75**
$2.0 \cdot 10^{-2}$	0.0271	**-7.44**	**11.34**

Although in this case no clear difference was observed between the constants calculated from the results obtained at the lowest or the highest bicarbonate concentrations, we maintained a consistency with the calculations made for soddyite and also in this case we only used the results obtained at the bicarbonate concentrations where the fourth U(VI) carbonate complex is the aqueous dominant species, marked in bold in Table 4-3. From the average of these results a solubility product for uranophane was calculated as:

$$\log K^0_{s0} = 11.7 \pm 0.6$$

This value has been compared with some solubility products of uranophane found in the literature. First of all, it must be stated the high discrepancy of values found, that go from the $\log K_{s0} = 9.4 \pm 0.5$ reported by Nguyen et al. (1992) to a $\log K_{s0} = 17.37$ found in the HATCHES database used by the HARPHRQ geochemical program. For the value reported by Nguyen et al. (1992), the same reluctances expressed above for their soddyite solubility product can be applied here. On the other hand, the value found in the HATCHES database is an old solubility constant extracted from a former EQ3/6 database. Compared to these values, the solubility product presented in this work falls in between, though it is certainly closer to the constant reported by Nguyen et al. (1992). In Figure 4-2 there is a comparison of the three models calculated with the solubility products presented in this work and the two values found in the literature, respectively, together with the solubilities reported in the experiments performed in this study.

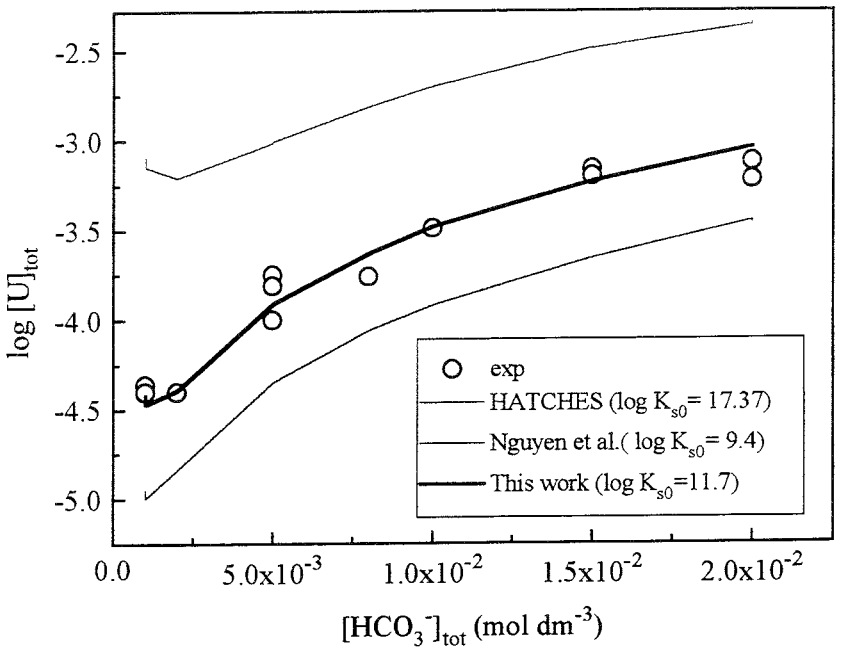

Figure 4-2. *Experimental solubilities obtained as a function of total bicarbonate concentration as well as calculated solubilities obtained by using different K_{S0} (see legend).*

4.2.2 Kinetics

The dissolution rates were in this case calculated from the least square regression of the initial linear trend of the uranium concentrations as a function of time. Taking into account the volume of the aqueous test solution, the rates were recalculated as moles of uranium per unit time, and subsequently normalized to the total surface area of solid used in the different runs. The calculated dissolution rates are presented in Table 4-4.

Table 4-4. Normalized release rates of U for uranophane.

$[HCO_3^-]$ (mol dm^{-3})	pH_0	Total surface area (m^2)	Rate (mol m^{-2} s^{-1})	log Rate
$1.0 \cdot 10^{-3}$	8.39	8.86	$7.68 \cdot 10^{-11}$	-10.11
$1.0 \cdot 10^{-3}$	9.24	8.86	$8.27 \cdot 10^{-11}$	-10.08
$2.0 \cdot 10^{-3}$	8.60	8.86	$1.09 \cdot 10^{-10}$	-9.96
$5.0 \cdot 10^{-3}$	8.69	8.86	$4.01 \cdot 10^{-11}$	-10.40*
$5.0 \cdot 10^{-3}$	8.62	8.86	$1.52 \cdot 10^{-10}$	-9.82
$5.0 \cdot 10^{-3}$	8.63	8.86	$4.29 \cdot 10^{-11}$	-10.37*
$8.0 \cdot 10^{-3}$	8.64	8.86	$4.01 \cdot 10^{-11}$	-10.40*
$1.0 \cdot 10^{-2}$	8.38	17.73	$4.20 \cdot 10^{-10}$	-9.38
$1.5 \cdot 10^{-2}$	8.60	8.86	$5.49 \cdot 10^{-10}$	-9.26
$1.5 \cdot 10^{-2}$	8.48	8.86	$3.48 \cdot 10^{-10}$	-9.46
$2.0 \cdot 10^{-2}$	8.52	17.73	$7.98 \cdot 10^{-10}$	-9.10
$2.0 \cdot 10^{-2}$	8.48	8.86	$4.70 \cdot 10^{-10}$	-9.33

From the analysis of the results obtained we have considered in this case the influence of both the bicarbonate and the proton concentration on the rate of dissolution. Hence, we postulated a dissolution rate equation of the form:

$$r = k \cdot [HCO_3^-]^m \cdot [H^+]^n \qquad \textbf{5-14}$$

The fitting was made by using the logarithmic form of equation (5-14):

$$\log r_0 = \log k + m \cdot \log [HCO_3^-]_0 + n \cdot \log [H^+]_0 \qquad \textbf{5-15}$$

Considering in all cases the initial rates of dissolution as well as the initial bicarbonate and proton concentrations (see Table 4-4), we obtained a good linear correlation, except for the data marked with an asterisk in Table 4-4, which were not used in the subsequent calculations. From the multivariate analysis of the data we obtained the following results:

$\log k = -9 \pm 2$

$m = 0.69 \pm 0.09$

$n = -0.1 \pm 0.2$

$r^2 = 0.93$

As observed, a bad definition is found for the proton concentration influence, though, due to the buffering of the test solutions because of the presence of bicarbonate, the pH varied only slightly from one experiment to another, which can be the reason for the observed lack of influence of this parameter. Anyway, the results obtained led us to the following final dissolution rate equation:

$$r_0 \text{ (mol m}^{-2}\text{ s}^{-1}) = 10^{-9 \pm 2} \cdot [HCO_3^-]^{0.69 \pm 0.09} \cdot [H^+]^{-0.1 \pm 0.2} \qquad \textbf{5-16}$$

By substituting the different values of both bicarbonate and proton concentrations that correspond to the different experiments performed, we found an initial dissolution rate that ranged from $1.2 \cdot 10^{-12}$ to $9.5 \cdot 10^{-12}$ mol m^{-2} s^{-1}. These dissolution rates are approximately between 600 and 100 times lower than the ones determined for soddyite (equation 5-9).

A comparison was made with the rate of dissolution determined for a natural sample of uranophane (Cera, 1996), where a synthetic granitic groundwater was used as a test solution, with a carbonate content of $3 \cdot 10^{-3}$ mol dm^{-3}. In that case, a dissolution rate of $6.6 \cdot 10^{-13}$ mol m^{-2} s^{-1} was obtained, that is, about ten times lower than the values determined in this study. However, this value falls between the ranges of uncertainty expressed in equation 5-16.

5 CONCLUSIONS

The dissolution behavior of soddyite and uranophane have been studied using two different main test solution compositions. In one case, carbonate free leaching solutions were employed, while in an other set of experiments different bicarbonate concentrations were added to the test solutions.

In the carbonate free experiments, precipitation of secondary phases took place in most of the experiments, both for soddyite and for uranophane, making basically unfeasible to extract useful information from these dissolution results. This behavior was not observed in the experiments performed in the presence of bicarbonate. It seems evident that the strong U(VI)-carbonate complexes stabilize uranium in solution. Hence, the thermodynamic and kinetic properties of soddyite and uranophane have then been determined in the presence of different bicarbonate concentrations, at 25°C. The test solutions were exposed to air throughout the experimental time.

The experimental data obtained at the end of the experiments carried out with soddyite correspond fairly well to the theoretical model calculated with a log K^0_{s0} of 3.9 ± 0.7. This value is approximately 1.5 orders of magnitude lower than the solubility product calculated by Nguyen et al. (1992) and Moll et al. (1996), while it corresponds fairly well with the value determined from a natural sample (Cera, 1996). Among the different possibilities that may account for these differences, we consider the fact that the value reported in Nguyen et al. (1992) and Moll et al. (1996) was extracted from a single experiment at pH=3 in both cases, which may involve a relatively large degree of uncertainty. Also, the presence of bicarbonate in our test solutions can also contribute to prevent the formation of possible secondary solid phases.

On the other hand, the general trend of the total uranium in solution measured in the experiments with soddyite as a function of time has been fitted by using a kinetic equation obtained from the principle of detailed balancing of the dissolution reaction. In addition, the EQ3/6 code has also been used to model the uranium concentrations as a function of time. Comparable results were obtained from both modeling exercises. The initial dissolution rate, normalized to the total surface area used in the experiments as measured with the BET method, gave an average value of 6.8 (±4.4) $\cdot 10^{-10}$ mol m^{-2} s^{-1}.

The data obtained for uranophane at the end of the experiments allowed the calculation of a solubility product for this phase of log K^0_{s0} = 11.7 ± 0.6. This constant falls between two values found in the literature: log K_{s0} = 9.4 ± 0.5 reported by Nguyen et al. (1992) and log K_{s0} = 17.37 found in the HATCHES database.

The kinetic treatment of the data has been made calculating the least square regression of the initial uranium concentrations determined a s a function of time. For this phase a clear dependence with the bicarbonate concentration has been found and a more ambiguous dependence with the proton concentration is also considered. A dissolution rate equation that fits most of the experiments performed has been derived:

$$r_0 \text{ (mol m}^{-2}\text{ s}^{-1}) = 10^{-9\pm2} \cdot [HCO_3^-]^{0.69\pm0.09} \cdot [H^+]^{-0.1\pm0.2}$$

6 REFERENCES

Bruno J. and Puigdomènech I., 1989. Validation of the SKBU1 uranium thermodynamic data base for its use in geochemical calculations with EQ3/6. Sci. Basis for Nucl. Waste Manag. XII, Ed. W. Lutze and R.C. Ewing, vol. 127, pp 887-896.

Casas I., Bruno J., Cera E., Finch R.J. and Ewing R.C., 1994. Kinetic and thermodynamic studies of uranium minerals. Assessment of the long-term evolution of spent nuclear fuel. SKB Technical Report TR 94-16.

Cera E., 1996. Estudis termodinàmics i cinètics de dissolució de fases naturals d'urani representatives d'un procés d'alteració oxidativa de l'òxid d'urani (IV). PhD Thesis.

de Pablo J., Duro L., Giménez J., Havel J., Torrero M.E. and Casas I., 1992. Fluorimetric determination of traces of uranium (VI) in brines and iron (III) oxides using separation on an activated silica gel column. Anal. Chim. Acta, Vol 264, pp 115.

Finch R.J. and Ewing R.C., 1989. Alteration of natural UO_2 under oxidizing conditions from Shinkolobwe, Katanga, Zaire: A natural analogue for the corrosion of spent fuel. SKB Technical Report TR 89-37.

Finch R.J. and Ewing R.C., 1991. Uraninite alteration in an oxidizing environment and its relevance to the disposal of spent nuclear fuel. SKB Technical Report TR 91-15.

Finch R.J. and Ewing R.C., 1992. The corrosion of uraninite under oxidizing conditions. J. of Nucl. Mat., Vol 190, pp 133-156.

Grenthe I., Fuger J., Konings R.J.M., Lemire R.J., Muller A.B., Nguyen-Trung C. and Wanner H., 1992. Chemical Thermodynamics of uranium (eds. Hans Wanner and Isabelle Forest). Elsevier Science Publishers B.V. The Netherlands.

Janeczek J. and Ewing R.C., 1992. Dissolution and alteration of uraninite under reducing conditions. J. of Nucl. Mat., Vol 190, pp 157-173.

Lasaga A.C., Berner R.A., Fisher G.W., Anderson D.E. and Kirkpatrick R.J., 1983. Kinetics of Geochemical Processes. Mineralogical Society of America, Reviews in Mineralogy Volume 8, Eds. A.C. Lasaga and R.J. Kirkpatrick.

Moll H., Geipel G., Matz W., Bernhard G. and Nitsche H., 1996. Solubility and speciation of $(UO_2)_2SiO_4{\cdot}2H_2O$ in aqueous systems. Radiochimica Acta, Vol 74, pp 3-7.

Nakamoto K., 1986. Infrared and Spectra of Inorganic and Coordination Compounds. J. Wiley and sons: New York.

Nguyen N., Silva R.J., Weed H.C. and Andrews JR. J.E., 1992. Standard Gibbs free energies of formation at the temperature 303.15 K of four uranyl silicates: soddyite, uranophane, sodium boltwoodite and sodium weeksite. J. Chem. Thermodynamics, Vol 24, pp 359-376.

Richard A. Nyquist and Ronald O. Kagel, 1971. Infrared Spectra of Inorganic Compounds. Academic Press: New York and London.

Rothenberg S.J., Flynn D.K., Eidson A.F., Mewhinney J.A. and Newton G.J., 1987. Determination of specific surface area by krypton adsorption, comparison of 3 different methods of determining surface area, and evaluation of different specific surface area standards. Journal of Colloid and Interface Science, Vol 116, pp 541-554.

Sing K.S.W., Everett D.H., Haul R.A.W., Moscou L., Pierotti R.A., Rouquerol J. and Siemieniewska T., 1985. Reporting physisorption data for gas/solid systems with special reference to the determination of specific area and porosity. Pure and Appl. Chem., Vol 57, pp 603-619.

List of SKB reports

Annual Reports

1977-78
TR 121
KBS Technical Reports 1 – 120
Summaries
Stockholm, May 1979

1979
TR 79-28
The KBS Annual Report 1979
KBS Technical Reports 79-01 – 79-27
Summaries
Stockholm, March 1980

1980
TR 80-26
The KBS Annual Report 1980
KBS Technical Reports 80-01 – 80-25
Summaries
Stockholm, March 1981

1981
TR 81-17
The KBS Annual Report 1981
KBS Technical Reports 81-01 – 81-16
Summaries
Stockholm, April 1982

1982
TR 82-28
The KBS Annual Report 1982
KBS Technical Reports 82-01 – 82-27
Summaries
Stockholm, July 1983

1983
TR 83-77
The KBS Annual Report 1983
KBS Technical Reports 83-01 – 83-76
Summaries
Stockholm, June 1984

1984
TR 85-01
Annual Research and Development Report 1984
Including Summaries of Technical Reports Issued during 1984. (Technical Reports 84-01 – 84-19)
Stockholm, June 1985

1985
TR 85-20
Annual Research and Development Report 1985
Including Summaries of Technical Reports Issued during 1985. (Technical Reports 85-01 – 85-19)
Stockholm, May 1986

1986
TR 86-31
SKB Annual Report 1986
Including Summaries of Technical Reports Issued during 1986
Stockholm, May 1987

1987
TR 87-33
SKB Annual Report 1987
Including Summaries of Technical Reports Issued during 1987
Stockholm, May 1988

1988
TR 88-32
SKB Annual Report 1988
Including Summaries of Technical Reports Issued during 1988
Stockholm, May 1989

1989
TR 89-40
SKB Annual Report 1989
Including Summaries of Technical Reports Issued during 1989
Stockholm, May 1990

1990
TR 90-46
SKB Annual Report 1990
Including Summaries of Technical Reports Issued during 1990
Stockholm, May 1991

1991
TR 91-64
SKB Annual Report 1991
Including Summaries of Technical Reports Issued during 1991
Stockholm, April 1992

1992
TR 92-46
SKB Annual Report 1992
Including Summaries of Technical Reports Issued during 1992
Stockholm, May 1993

1993
TR 93-34
SKB Annual Report 1993
Including Summaries of Technical Reports Issued during 1993
Stockholm, May 1994

1994

TR 94-33

SKB Annual Report 1994

Including Summaries of Technical Reports Issued during 1994

Stockholm, May 1995

1995

TR 95-37

SKB Annual Report 1995

Including Summaries of Technical Reports Issued during 1995

Stockholm, May 1996

1996

TR 96-25

SKB Annual Report 1996

Including Summaries of Technical Reports Issued during 1996

Stockholm, May 1997

List of SKB Technical Reports 1997

TR 97-01

Retention mechanisms and the flow wetted surface – implications for safety analysis

Mark Elert

Kemakta Konsult AB

February 1997

TR 97-02

Äspö HRL – Geoscientific evaluation 1997/1. Overview of site characterization 1986–1995

Roy Stanfors[1], Mikael Erlström[2], Ingemar Markström[3]

[1] RS Consulting, Lund

[2] SGU, Lund

[3] Sydkraft Konsult, Malmö

March 1997

TR 97-03

Äspö HRL – Geoscientific evaluation 1997/2. Results from pre-investigations and detailed site characterization. Summary report

Ingvar Rhén (ed.)[1], Göran Bäckblom (ed.)[2], Gunnar Gustafson[3], Roy Stanfors[4], Peter Wikberg[2]

[1] VBB Viak, Göteborg

[2] SKB, Stockholm

[3] VBB Viak/CTH, Göteborg

[4] RS Consulting, Lund

May 1997

TR 97-04

Äspö HRL – Geoscientific evaluation 1997/3. Results from pre-investigations and detailed site characterization. Comparison of predictions and observations. Geology and mechanical stability

Roy Stanfors[1], Pär Olsson[2], Håkan Stille[3]

[1] RS Consulting, Lund

[2] Skanska, Stockholm

[3] KTH, Stockholm

May 1997

TR 97-05

Äspö HRL – Geoscientific evaluation 1997/4. Results from pre-investigations and detailed site characterization. Comparison of predictions and observations. Hydrogeology, groundwater chemistry and transport of solutes

Ingvar Rhén[1], Gunnar Gustafson[2], Peter Wikberg[3]

[1] VBB Viak, Göteborg

[2] VBB Viak/CTH, Göteborg

[3] SKB, Stockholm

June 1997

TR 97-06

Äspö HRL – Geoscientific evaluation 1997/5. Models based on site characterization 1986–1995

Ingvar Rhén (ed.)[1], Gunnar Gustafson[2], Roy Stanfors[4], Peter Wikberg[4]

[1] VBB Viak, Göteborg

[2] VBB Viak/CTH, Göteborg

[3] RS Consulting, Lund

[4] SKB, Stockholm

May 1997

TR 97-07

A methodology to estimate earthquake effects on fractures intersecting canister holes

Paul La Pointe, Peter Wallmann, Andrew Thomas, Sven Follin

Golder Associates Inc.

March 1997

TR 97-08

Äspö Hard Rock Laboratory Annual Report 1996

SKB

April 1997

TR 97-09

A regional analysis of groundwater flow and salinity distribution in the Äspö area

Urban Svensson

Computer-aided Fluid Engineering AB

May 1997

TR 97-10

On the flow of groundwater in closed tunnels. Generic hydrogeological modelling of nuclear waste repository, SFL 3–5

Johan G Holmén
Uppsala University/Golder Associates AB
June 1997

TR 97-11

Analysis of radioactive corrosion test specimens by means of ICP-MS. Comparison with earlier methods

R S Forsyth
Forsyth Consulting
July 1997

TR 97-12

Diffusion and sorption properties of radionuclides in compacted bentonite

Ji-Wei Yu, Ivars Neretnieks
Dept. of Chemical Engineering and Technology, Chemical Engineering, Royal Institute of Technology, Stockholm, Sweden
July 1997

TR 97-13

Spent nuclear fuel – how dangerous is it? A report from the project "Description of risk"

Allan Hedin
Swedish Nuclear Fuel and Waste Management Co, Stockholm, Sweden
March 1997

TR 97-14

Water exchange estimates derived from forcing for the hydraulically coupled basins surrounding Aspö island and adjacent coastal water

Anders Engqvist
A & I Engqvist Konsult HB, Vaxholm, Sweden
August 1997